Journal of Inorganic Biochemistry 236 (2022) 111975

Contents lists available at ScienceDirect

Journal of Inorganic Biochemistry

journal homepage: www.elsevier.com/locate/jinorgbio

Antitumor activity of copper(II) complexes with Schiff bases derived from N′-tosylbenzene-1,2-diamine

María Diz [a], María L. Durán-Carril [a], Jesús Castro [b,*], Samuel Alvo [c], Lucía Bada [c], Dolores Viña [c], José A. García-Vázquez [a,*]

[a] Departamento de Química Inorgánica, Campus Vida, Universidad de Santiago de Compostela, 15782 Santiago de Compostela, Spain
[b] Departamento de Química Inorgánica, Facultade de Química, Edificio de Ciencias Experimentais, Universidade de Vigo, 36310 Vigo (Galicia), Spain
[c] CIMUS, Campus Vida, Universidad de Santiago de Compostela, 15782 Santiago de Compostela, Spain

ARTICLE INFO

Keywords:
Copper
Schiff bases ligands
Electrochemical synthesis
Structure elucidation
Hydrogen bonds
Stacking interactions
Antitumoral activity

ABSTRACT

The electrochemical oxidation of anodic metal copper in a solution of the ligands N-[(5-*tert*-butyl-2-hydroxyphenyl)methylidine]-N′-tosylbenzene-1,2-diamine [H_2L^1] and N-[(3,5-di-*tert*-butyl-2-hydroxyphenyl)methylidine]-N′-tosylbenzene-1,2-diamine, [H_2L^2] afforded homoleptic [CuL] compounds or solvate [CuLS] complexes. The addition to the electrochemical cell of coligands (L') such as 2,2′-bipyridine (2-bpy), 4,4′-bipyridine(4-bpy) or 1,10-phenanthroline (phen) allowed the synthesis, in one step, of heteroleptic [CuLL'] compounds, namely [$CuL^1(H_2O)$] **(1)**, [CuL^1(2,2′-bpy)]·CH_3CN **(2)**, [CuL^1(phen)]·H_2O **(3)**, [$Cu_2L^1_2$(4,4′-bpy)] **(4)**, [$CuL^2(CH_3OH)$] **(5)**, [CuL^2(2,2′-bpy)] **(6)**, [CuL^2(phen)] **(7)** and [$Cu_2L^2_2$(4,4′-bpy)] **(8)**. The crystal structures of both ligands, H_2L^1, H_2L^2, and those of the complexes **(2)**, **(4)**, **(5)**, **(6)** and **(7)** have been determined by X-ray diffraction techniques. Coordination polyhedron around metal atom is square planar for [$CuL^2(CH_3OH)$] **(5)** and [$Cu_2L^1_2$(4,4′-bpy)] **(4)** and square pyramid for the other complexes with additional chelating ligands. The cytotoxic activity of this new series of copper(II) complexes against the SH-SY5Y neuroblastoma cell line and U87-MG and U373-MG glioblastoma cell lines has been investigated. Most of the test compounds showed higher activity than cisplatin in the three cell lines. Among this series, compound [CuL^1(phen)] **(3)** displayed the highest activity with IC_{50} equal to 1.77 μM on SH-SY5Y whereas compound [$Cu_2L^1_2$(4.4′-bpy)] **(4)** resulted the most potent compounds on U87 MG and U373 MG glioblastoma cell lines. Studies on the cytotoxic activity of these derivatives suggest that these compounds induce cell death by a mechanism other than apoptosis.

1. Introduction

Cancer is a disease with one of the highest mortality rates affecting the worldwide population. It was computed about 18.1 million new cancer cases and 9.6 million cancer deaths happened in 2018 worldwide [1]. Probably, the mortality will be about 16.3 million (9.2 males and 7.1 females) in 2040 [2]. Therefore, the design and development of effective anticancer drugs is one of the most important areas of research. One of the most interesting lines is medicinal inorganic chemistry or the chemistry of metal based drugs, since offers additional chances for the design of new therapeutic agents [3]. This area began with the serendipitous Rosenberg's discovery of the activity of cisplatin. The action mechanism of platinum-based therapeutics seems to be the bonding to nitrogen atoms on adjacent DNA bases [4]. These interactions interfere with the binding of essential proteins for transcription and produces an attenuation of the grown of cancerous cells. However, the clinical use of these drugs is restricted by several side effects including nephrotoxicity and neurotoxicity, or even by acquired resistance to platinum-based drugs [5–8]. Although there are several approved platinum-based drugs (cisplatin, carboplatin, oxaliplatin, LA-12 or dicycloplatin), and also there are several are under Clinical Trial Application ("CTA") for evaluation, research about new compounds (and also new formulations) continues [9–10]. A big amount of new research is ongoing by using other approaches [11]. One of the most extended strategies is to use another metal center [12–15]. Several metals were tested, [16–18] sometimes because their complexes can bind to DNA or other action similar to classical platinum(II) therapeutic compounds, and also by their redox properties. In the last field, at least Co(III), Fe(III), Pt(IV), Ru (III/II), Os(II), and Ir(III) complexes have been recently studied [19].

Among new metal-base drugs different from Pt, one of the more

* Corresponding authors.
E-mail address: jesusc@uvigo.gal (J. Castro).

https://doi.org/10.1016/j.jinorgbio.2022.111975
Received 13 July 2022; Received in revised form 10 August 2022; Accepted 18 August 2022
Available online 24 August 2022

promising is copper(II) [20–29]. By one hand, copper is an essential element for most aerobic organisms, and consequently it has a well-established homeostasis procedure, so their toxicity could be naturally controlled [30–32]. Copper(II) ion is also interesting due its bioavailability, since copper is present as cofactor in many enzymes. It is involved in several processes as hemoglobin formation, carbohydrates metabolism, catecholamine biosynthesis, or reducing the production of reactive oxygen species (ROS). In addition, the observation of increased copper levels in cancer tissue, prompted to study its anticancer activity due perhaps it would be easy the increasing of its concentration in the target organ. The cytotoxic activity of copper(II) complexes comes from two principal sources on depending on their structure [25]. Some of them interact with DNA with several intensities, from strong covalent bonding, simple intercalation or hydrogen bonding. But some of them also show DNA cleavage activity, and also on two possible targets, on the phosphate backbone as consequence of the Lewis acidity or due the oxidative properties of copper(II) acting on the sugar and base moieties [33].

We have a long standing interest in copper(II) complexes with Schiff bases [34–36] and also with amide ligands. The use of salicyaldehyde derived Schiff bases with N, O donor sets plays an important role in coordination chemistry related to enzymatic reactions that may be potentially used for many biological applications [37]. One particular class of amide ligands is represented by the sulfonamide ligands [35,36]. In this paper we synthetized a couple of ligands combining one salicylaldimine group together with a tosylimine one (see Scheme 1). This combination produces a potentially tridentated NNO ligand. Interest in the synthesis of metal complexes with these ligands arises, in part, from the fact that they can easily be made due the electron-withdrawing effect of the sulfonyl substituent, which increases the acidic character of the NH group and makes the process of ligand deprotonation easier [35,36,38]. Furthermore, variation of the substituents in these ligands is facile. This latter feature provides the possibility of tailoring the bite angle and degree of steric hindrance present in the ligand and, in addition, it is believed that the presence of bulky substituents on these ligands stabilizes the metal complexes. The anticancer activity of such kind of κ^3-N,N′,O complexes is well stablished [26], both for tetra-coordinated copper(II) complexes, where the additional ligand is chloride, water, or other monodentated ligands, as well for the complexes with high coordination number bearing additional κ^2-N,N′ ligand as 2,2′-bipyridine or 1,10-phenantroline [25,26,39–42].

Moreover, these complexes were synthesized by an electrochemical procedure in which the metal is the anode of an electrochemical cell [42]. This procedure represents a simple, high-yielding alternative to other standard chemical procedures. Among the benefits of this technique is the isolation of neutral pure complexes, without the presence of any anion, and also the rate and purity of the compounds obtained in a one-pot experiment.

Cytotoxic activity of this new series of copper(II) complexes with the Schiff bases derivatives of *N*-tosylbenzene-*N*′-2-hydroxyphenylmethylidine-1,2-diamine was evaluated in the SH-SY5Y neuroblastoma and U87-MG and U373-MG glioblastoma cell lines and MRC-5 fibroblast cells. Furthermore, [$CuL^1(H_2O)$] **(1)**, [CuL^1(phen)] **(3)** and [$Cu_2L^1_2$(4,4′-bpy)] **(4)** that exhibited the most potent activity were investigated by their mechanism of action by modifying the ROS generation and expression of apoptosis-related proteins.

2. Experimental section

2.1. Materials

2.1.1. General synthesis

All solvents, 1,2-phenylendiamine, 4-toluensulfonyl chloride, 3-*tert*-butyl-2-hydroxy-benzaldehyde and 3,5-di-*tert*-butyl-2-hydroxy-benzaldehyde were commercial products (Aldrich Chemie) and were used as supplied. Copper (Ega Chemie) was used as plates (ca. 2 × 2 cm). *N*-tosyl-1,2-diaminobenzene was prepared following the general procedure described by Malik [43].

2.2. Instrumental

Microanalyses were performed using a PerkinElmer 240B microanalyzer. IR spectra were recorded as KBr mulls on a Bruker IFS-66 *V* spectrophotometer. The ^{1}H and ^{13}C NMR spectra of the ligand were recorded on a Bruker WM 350 MHz spectrophotometer using the DMSO-d_6 solvent. The chemical shifts were recorded against TMS as the internal standard. IE and FAB mass spectra were recorded on Hewlet-Packard HP5988A and Micromass Autospec instruments, using 3-nitrobenzyl alcohol (3-NBA) as the matrix material for the FAB spectra. Solid-state electronic spectra (UV–Vis) were measured on UV-3101 PC Shimadzu diffuse reflectance spectrophotometer.

2.2.1. Crystal structure determinations

The data collections were taken on a MACH3 Enraf Nonius with graphite-monochromated Cu-K_α radiation or in a Bruker Smart CCD area-detector diffractometer with graphite-monochromated Mo-K_α radiation. Absorption corrections were carried out using SADABS [44]. The crystallographic treatment was performed with the Oscail program [45], solved using the SHELXT program [46]. The structure was subsequently refined by a full-matrix least-squares based on F^2 using the SHELXL program [47]. Non-hydrogen atoms were refined with anisotropic displacement parameters. Hydrogen atoms for complexes were included in idealized positions and refined with isotropic displacement parameters. Details of crystal data and structural refinement are given in Table S1 in the Supplementary Material. CCDC 2180885 to 2180892 contain the supplementary crystallographic data for this paper. These

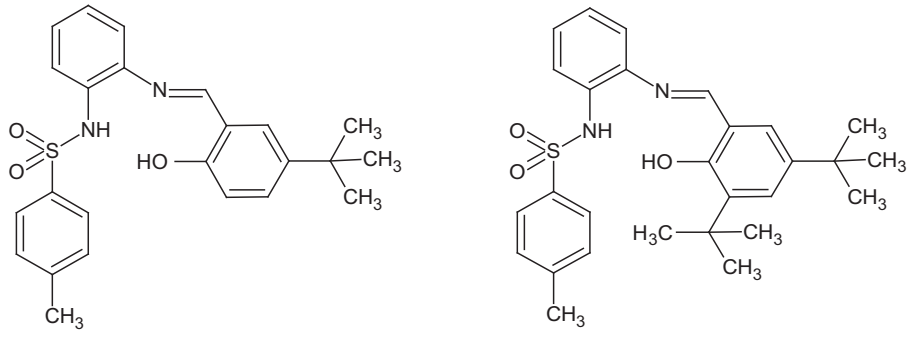

Scheme 1. General structural formulae for the ligands H_2L^1 and H_2L^2.

data can be obtained free of charge from the Cambridge Crystallographic Data Centre via www.ccdc.cam.ac.uk/data_request/cif

2.3. Synthesis of the ligands and the copper(II) complexes

2.3.1. Synthesis of N-[(5-tert-butyl-2-hydroxyphenyl)methylidine]-N′-tosylbenzene-1,2-diamine (H_2L^1)

The ligand [H_2L^1] was prepared following a standard Schiff base procedure by condensation between *N*-tosyl-1,2-diaminobenzene (2.840 g, 10.83 mmol) and 5-*tert*-butyl-2-hydroxy-benzaldehyde (2.0 mL 11.66 mmol) in methanol (60 mL). The solution was heated under reflux for 5 h. The slow evaporation of the methanol solution afforded suitable yellow crystals of H_2L^1 useful for X-ray studies. They were isolated by filtration, washed with methanol and ether and dried. Yield: 3.548 g, 8.40 mmol (78%) Elemental analysis calc. (%) for $C_{24}H_{26}N_2O_3S$ (422.53): C, 68.22; H, 6.20, N, 6.63; S, 7.59. Found: 68.15; H, 6.39, N, 6.69; S, 7.14. IR (KBr, cm^{-1}): 3500(m, br), 3257(m), 2963(m), 1615(s), 1575(m), 1489 (s), 1408(m), 1340(s), 1283(m), 1253(m), 1166(s), 1092 (m), 803(m), 669(m). ^1H NMR (DMSO-d,^{6} ppm): 11.54 (s, 1H, NH), 9.78 (s, 1H, OH), 8.20 (s, 1H, HC═N), 7.60–6.90 (m, 11H, phenyl), 2.10 (s, 3H, CH_3), 1.29 (s, 9H, ^{t}Bu). ^{13}C NMR (DMSO-d,^{6} ppm): 198 (*C*=N); 100–170 [Arom., 163 (*C*-NH-SO_2-), 170 (*C*-OH)]; 39 (CH_3); 37 (C(*CH_3*)); 27 (*C*(CH_3)) MS(EI) *m/z*: 422 [H_2L^1], 267 [H_2L^1]-Ts, 155 Ts.

2.3.2. Synthesis of N-[(3,5-di-tert-butyl-2-hydroxyphenyl)methylidine]-N′-tosylbenzene-1,2-diamine, (H_2L^2)

The ligand [H_2L^2] was prepared following a similar procedure, by condensation between N-tosyl-1,2-diaminobenzene (2.740 g, 10.44 mmol) and 3,5-di-*tert*-butyl-2-hydroxy-benzaldehyde (2.473 g 10.45 mmol) in methanol (60 mL). The solution was heated under reflux for 5 h. The resulting yellow precipitate was filtered off, washed with ethanol and ether and dried, and recrystallized in methanol. The slow evaporation of the methanol solution afforded suitable yellow crystals of H_2L^2 suitable for X-ray studies. Yield: 3.789 g, 7.92 mmol. (76%). Elemental analysis calc. (%) for $C_{28}H_{34}N_2O_3S$ (478.61): C, 70.27; H, 7.15, N, 5.85, S, 6.70. Found: 69.62; H, 7.16, N, 5.82, S, 6.58. IR (KBr, cm^{-1}): 3480(m, br), 3247(m), 2954(m), 1614(s), 1581(m), 1492(m), 1396(m), 1340(s), 1271(m), 1168(vs), 1092(m), 683(m). ^1H NMR (DMSO-d,^{6} ppm): 11.69 (s, 1H, NH), 9.87 (s, 1H, OH), 8.20 (s, 1H, HC═N), 8.0–6.0 (m, 10H, phenyl), 2.10 (s, 3H, CH_3), 1.47 (s, 9H, ^{t}Bu), 1.29 (s, 9H, ^{t}Bu). ^{13}C NMR (DMSO-d,^{6} ppm): 207 (*C*=N); 100–167 [Arom., 157 (*C*-NH-SO_2-), 167 (*C*-OH)]; 22 (CH_3); 34–36(C(*CH_3*)); 30–32 (*C*(CH_3)). MS(EI) *m/z*: 478 [H_2L^1], 323 [H_2L^1]-Ts, 155 Ts.

Their structural formulae are depicted in Scheme 1.

2.3.3. Electrochemical synthesis of the copper(II) complexes

The copper complexes were obtained using an electrochemical procedure [42]. The cell consisted of a tall-form beaker (100 mL) fitted with a rubber bung through which the electrochemical leads entered. An acetonitrile solution of the ligand and the eventual coligand (2,2′-bpy, 4,4′-bpy or phen), containing a small amount of tetramethylammonium perchlorate as a current carrier (about 10 mg), was electrolyzed using a platinum wire as the cathode and a metal plate as the sacrificial anode (*Caution*: Although problems were not encountered in this work, all perchlorate compounds are potentially explosive, and should be handled in small quantities and with great care!). The applied voltages (10–20 *V*) allowed sufficient current flow for smooth dissolution of the metal. The current was maintained at 10 mA. In all cases, during the electrolysis hydrogen was evolved at the cathode. Under these conditions the cell can be summarized as Cu(+)/H_2L + CH_3CN + L'/Pt(−).

Synthesis of [CuL^1(H_2O)] (**1**)**.** A solution of H_2L^1 (0.150 g, 0.355 mmol) in acetonitrile (50 mL), was electrolyzed for 0.833 h with a current of 10 mA and 20.4 mg of the metal were dissolved from the anode, E_f = 1.03 mol·F^{-1}. The green reaction mixture is filtered to remove any impurities and allowed to air concentrate at room temperature resulting in a green solid that is filtered, washed with acetonitrile and ether and dried under vacuum and characterized as [$CuL^1(H_2O)$]. Yield: 0.153 g, 0.305 mmol, 86%. Elemental analysis calc. (%) for $C_{24}H_{26}CuN_2O_4S$ (502.06): C, 57.41; H, 5.21; N, 5.58, S, 6.39. Found: C, 57.23; H, 5.55; N, 5.86, S 6.10. IR (KBr, cm^{-1}): 3380(m,br), 1616(vs), 1531(m), 1484(s), 1411(s), 1380(m), 1363(m) 1300(s), 1258(vs), 1163 (m), 1135(s), 1086(m), 963(s), 836(m), 742(m). MS(FAB) *m/z*: 969 [$Cu_2L^1_2$] 814 [$Cu_2L^1(L^1$-Ts)], 483 [CuL^1], 329 [CuL^1-Ts]. UV (cm^{-1}): 15480.

Synthesis of [CuL^1(2,2′-bpy)]·CH_3CN (**2**). A solution of H_2L^1 (0.151 g, 0.360 mmol) and 2,2′-bipyridine (0.060 g, 0.384 mmol) in acetonitrile (50 mL) was electrolyzed 0.833 h at 10 mA, so 19.1 mg of the metal were dissolved from the anode, E_f = 0.97 mol·F^{-1}. The green solution obtained was allowed to air concentrate to room temperature. Green crystals of [CuL^1(2,2′-bpy)]. CH_3CN (**2**) suitable for X-ray studies were obtained for crystallization. (Yield: 0.152 g, 0.223 mmol, 62%). Elemental analysis calc. (%) for $C_{36}H_{35}CuN_5O_3S$ (681.29): C, 63.46; H, 5.18; N, 10.28, S 4.70. Found: C, 63.58; H, 4.91; N, 9.82, S 4.87. IR (KBr, cm^{-1}): 1616(vs), 1525(m), 1482(s), 1449(s), 1379(m), 1323 (m), 1309 (w), 1301(m), 1222(s), 1142(s), 1087(s), 949(m), 770(m), 745(m). MS (FAB) *m/z*: 639 [CuL^1(2,2′-bpy)], 483 [CuL^1]. UV (cm^{-1}): 10820 and 15060.

Synthesis of [CuL^1(phen)]·H_2O (**3**)**.** Green needles of [CuL^1(phen)]·H_2O were obtained by electrochemical oxidation of copper metal in a cell containing the ligand H_2L^1 (0.150 g, 0.355 mmol) and 1,10-phenanthroline (0.070 g, 0.388 mmol) in acetonitrile (50 mL), during 0.833 h at 10 mA. Under these conditions, 19.2 mg of the metal were dissolved from the anode. E_f = 0.97 mol·F^{-1}. After air concentrate, the needles were isolated by filtration, washed with acetonitrile and ether and dried under vacuum. Yield: 0.169 g, 0.248 mmol, 70%. Elemental analysis calc. (%) for $C_{36}H_{34}CuN_4O_4S$ (682.29): C, 63.37; H, 5.02; N, 8.21; S, 4.70. Found: C, 63.34; H, 5.12; N, 8.56; S, 4.45. IR (KBr, cm^{-1}): 1616 (vs), 1520(m), 1480(s), 1461(s), 1427(s), 1379(m), 1364(m), 1323(m), 1297(m), 1253(s), 1166(m), 1142(s), 1090(m), 968(s), 842(m), 727(m). MS(FAB) *m/z*: 663 [CuL^1(phen)]. UV (cm^{-1}), 10707 and 14620.

Synthesis of [Cu$_2$L$^1_2$(4,4′-bpy)] (**4**)**.** A solution of H_2L^1 (0.151 g, 0.357 mmol) and 4,4′-bipyridine (0.059 g, 0.378 mmol) in acetonitrile (50 mL) was electrolyzed during 0.833 h at 10 mA and 18.7 mg of the metal were dissolved from the anode, E_f = 0.95 mol.F^{-1}. The resulting solution was air concentrated at room temperature and the solid obtained was filtered, washed with water, then with acetonitrile and ether and dried under vacuum. Crystals appropriate of (**4**) were used for X-ray diffraction studies. Yield: 0.180 g, 0.321 mmol, 90%. Elemental analysis calc. (%) for $C_{29}H_{28}CuN_3O_3S$ (562.14): C, 61.96; H, 5.02; N, 7.47, S 5.70. Found: C, 61.68; H, 5.07; N, 7.77; S, 5.68. IR (KBr, cm^{-1}): 1616(vs), 1601(m), 1525(m), 1480(s), 1412(s), 1381(m), 1319(m), 1299(s), 1256 (m), 1220(s), 1170 (m), 1140(s), 187(m), 1019(m), 957(m), 811(m), 745(m). MS(FAB) *m/z*: 640 [CuL^1(4,4′-bpy)], 483 [CuL^1], 329 [CuL^1]-Ts. UV(cm^{-1}): 15060.

Synthesis of [CuL^2(CH_3OH)] (**5**). This complex was prepared following a similar experiment to that describe above. A solution of H_2L^2 (0.150 g, 0.313 mmol) in acetonitrile (50 mL) was electrolyzed (10 mA during 0.833 h), leading to the dissolution of 20.7 mg from the anode, E_f = 1.05 mol·F^{-1}. The initial yellow solution becomes dark green during the electrolytic process. At the end of the electrolysis the resulting solution was filtered to remove insoluble impurities and concentrated at room temperature to give a green solid. The crystallization of the resulting green solid from methanol gave green crystals suitable for X-ray diffraction studies. The solid was filtered, washed with acetonitrile and dried and characterized as [CuL^2(CH_3OH)] (**5**). Yield: 0.132 g, 0.231 mmol, 74%. Elemental analysis calc. (%) for $C_{29}H_{36}CuN_2O_4S$ (572.22): C, 60.87; H, 6.34; N, 4.89, S 5.60; found C, 60.34; H, 6.68; N, 4.51, S 5.06. IR (KBr, cm^{-1}): 3417(m, br), 1613(s), 1527(s), 1484(m), 1458(m), 1387(s), 1361(m), 1296(s), 1255(s), 1188(s), 1163 m), 1126 (s), 1087(m), 954(vs), 739(m). MS(FAB) *m/z*: 541 [CuL^2], 323 [L^{2-}Ts]. UV (cm^{-1}): 15198.

Synthesis of [CuL^2(2,2′-bpy)] (**6**)**.** A solution of H_2L^2 (0.150 g, 0.313

mmol) and 2,2′-bipyridine (0.050 g, 0.32 mmol) in acetonitrile (50 mL) was electrolyzed for 0.833 h with a current of 10 mA, provoking the dissolution of 18.7 mg of the metal from the anode. $E_f = 0.95$ mol·F^{-1}. The resulting solution was allowed to air concentrate giving green crystals of [CuL^2(2,2′-bpy)] (**6**) suitable for X-ray diffraction analysis. Yield: 0.187 g, 0.269 mmol, 86%. Elemental analysis calc. (%) for $C_{38}H_{40}CuN_4O_3S$ (696.3): C, 65.55; H, 5.78; N, 8.05, S 4.61; found C, 65.38; H, 5.93; N, 8.02, S 4.35. IR (KBr, cm^{-1}): 1606(s), 1543(s), 1426 (m), 1364(m), 1297(m), 1252 (m), 1160(m), 1139(vs), 1089(s), 951(m), 833(m), 809(m), 762(s), 740(m). MS(FAB) *m/z*: 695 [CuL^2(2,2′-bpy)], 541 [CuL^2]. UV (cm^{-1}): 11010, 15240.

Synthesis of [CuL^2(phen)] (**7**). A solution of H_2L^2 (0.150 g, 0.313 mmol) and 1,10-phenanthroline (0.062 g, 0.344 mmol) in acetonitrile (50 mL) was electrolyzed during 0.833 h at 10 mA, causing 21.6 mg of the metal from the anode to dissolve. $E_f = 1.09$ mol·F^{-1}. Air concentration of the resulting solution provided a dark oil, which was redissolved with diethyl ether. The final solid was washed with water to remove the possible perchlorate present, filtered, washed again with water and ether, dried in vacuum and characterized as [CuL^2(phen)]. An acetonitrile solution of this solid afforded crystals useful for X-ray diffraction studies after slow evaporation. Yield: 0.200 g, 0.278 mmol, 89%. Elemental analysis calc. (%) for $C_{40}H_{40}CuN_4O_3S$ (720.36): C, 66.60; H, 5.60; N, 7.78; S, 4.45; found C, 66.10; H, 5.49; N, 7.88; S, 4.13. IR (KBr, cm^{-1}): 1608(s), 1588(s), 1522(m), 1483(m), 1429(s), 1385(s), 1361(m), 1331(m), 1309(s), 1277(s), 1161(m), 1141(s), 1089(m), 952 (s), 845(m), 812(m), 744(m), 723(s). MS(FAB) *m/z*: 719 [CuL^2(phen)], 541 [CuL^2]. UV(cm^{-1}): 11430, 15385.

Synthesis of [Cu$_2$L$^2_2$(4,4′-bpy)] (**8**). A solution of H_2L^2 (0.150 g, 0.313 mmol) and 4,4′-bipyridine (0.050 g, 0.32 mmol) in acetonitrile (50 mL) was electrolyzed for 0.833 h with a current of 10 mA, which caused 19.8 mg of the metal from the anode to dissolve. $E_f = 1.00$ mol·F^{-1}. The resulting solution was allowed to air concentrate at room temperature and the green precipitate obtained was washed with water, acetonitrile and ether and dried in vacuum. Yield: 0.167 g, 0.269 mmol, 86%. Elemental analysis calc. (%) for $C_{33}H_{36}CuN_3O_3S$ (618.3): C, 63.90; H, 6.17; N, 6.77, S 5.17; found C, 63.55; H, 5.76; N, 7.08; S, 4.94. IR (KBr, cm^{-1}): 1609(s), 1588(m), 1527(s), 1482(m), 1424(m), 1385(m), 1360 (w), 1322(m), 1297(m), 1252(m), 1162(m), 1136(s), 1089(m), 1020 (m), 960(m), 836(m), 809(m), 786(m), 744(m). MS(FAB) *m/z*: 696 [CuL^2(4,4′-bpy)], 479 L^2. UV (cm^{-1}): 15385.

2.4. Cytotoxicity studies

2.4.1. Cell culture

Human neuroblastoma SH-SY5Y cells (American Type Culture Collection ATCC) were maintained in a 1:1 mixture of Ham's F12:Dulbecco's Modified Eagle's Medium (DMEM) supplemented with L-glutamine (2 mM), nonessential aminoacids (1%), fetal bovine serum (FBS, 10% *v/v*), penicillin (100 IU/mL) and streptomycin (100 μg/mL) [48].

Human glioblastoma U87-MG and U373-MG cells (American Type Culture Collection ATCC) were maintained in DMEM Low glucose (1 g/L) supplemented with fetal bovine serum (FBS, 10% v/v), penicillin (100 IU/mL) and streptomycin (100 μg/mL) [49].

Mortal human MRC5 fibroblasts were maintained in MEM supplemented with fetal bovine serum (FBS, 10% v/v), penicillin (100 IU/mL) and streptomycin (100 μg/mL).

The different cell lines were grown in 10 cm diameter plastic plates under controlled conditions (a humid atmosphere of 5% CO_2 at 37 °C) in an incubator (Binder CB150). Culture medium was replaced every 2 days, and, at 80–90% of confluence, the cells were sub-cultured.

2.4.2. Cell treatment and analysis of viability

Copper(II) complex were dissolved in DMSO to obtain 5 mM stock solutions and diluted in medium in the same day of the experiment to adjust the final concentration of DMSO so that do not exceed 0.5% (*v*/v) in cell cultures.

The cytotoxic activity of copper(II) complex was measured in vitro in SH-SY5Y, U87-MG, U373-MG and MRC5 cells using the 3-[4,5-dimethylthiazole-2-yl]-2,5-dimethyltetrazolium bromide (MTT) assay [50]. Cells were seeded in 96-well plates at 1×10^4 cells/well and grown to confluence. Copper(II) complexes **(1–8)** at a range of concentrations (0.5–50 μM) were added to the medium and cells were incubated for 24 h. After this incubation, 10 μL of MTT (5 mg/mL) was added to each well and further incubated for 2 h at 37 °C. Then, culture medium was removed, 100 μL DMSO/well was added to solve the formazan crystals formed by the viable cells and the absorbance (λ 540 nm) was quantified in a plate reader (Fluo-star OptimaTM, BMG LABTECH). The viability (percentage) was calculated as [Absorbance (treatment)/Absorbance (negative control)]100%.

2.4.3. Intracellular ROS measurements

Intracellular ROS generation was measured in vitro using 5-(and-6)-carboxy-2′,7′-dichlorofluorescein diacetate (carboxy-DCFDA). Cells (1×10^4/well) were seeded in a 96-well black/clear bottom plate and grown for 24 h. The copper(II) complexes **1**, **3** and **4** or vehicle (DMSO) were added to the medium and cells were incubated for 24 h under standard conditions (37 °C, 5% CO_2). After 24 h, the medium was removed, and the cells were washed with PBS. 100 μL of medium containing cDCFDA probe (5 μM) was added in each well and the cells were again incubated for 30 min. At the end of this time, the medium was removed and the cells were washed with PBS. 100 μL of Hank's were added to each well and the cells were again treated with the copper(II) complexes **1**, **3** and **4** or DMSO. Increase in fluorescence was determined during a period of 2 h in 5 min intervals (λ excitation 485 nm, λ emission 520 nm) at 37 °C in a fluorescence reader plate (Fluo-star OptimaTM, BMG LABTECH) [51].

ROS were determined by calculating the area under the curve (AUC) obtained by representing the fluorescence generated (Y axis) versus time (X axis) for the different treatments. Each experiment was performed in triplicate. In the bar graph, the different treatment groups were represented on the abscissa axis and the percentage of AUC for each of the groups versus the AUC corresponding to the control (100%) on the ordinate axis. The results represent the mean ± standard error of the mean (s.e.m.) of 3 experiments ($n = 3$). Data were analyzed via one-way analysis of variance (ANOVA) followed by Bonferroni's multiple comparison test.

2.4.4. Western blot

Cells were seeded in 6 well plates at a density of 1.5×10^4 cells/cm^2. Reached the confluence U87-MG cells were treated with complex **1** (10 μM), SH-SY5Y cells with **3** (1.77 μM) and U373-MG cells with **4** (10 μM) for 24 h at 37 °C. After 24 h incubation, cells were homogenized in lysis buffer containing 50 mM Tris-HCl (pH 7.5), 150 mM NaCl, 1 mM ethylenediamine tetraacetic acid (EDTA), 1% Triton X-100 and protease inhibitor cocktail [4 mM phenylmethanesulfonyl fluoride (PMSF), 20 mM Na_3VO_4, 20 mM NaF and 50 μg/mL aprotinin]. The samples were centrifuged at 11,200*g* (4 °C) for 15 min. After supernatants were harvested, they were centrifuged again for 8 min under the same conditions. Protein concentration was determined with Bio-Rad Protein Assay Dye Reagent (Bio-Rad Laboratories GmbH), according to manufacturer's protocol. Proteins (20 μg) were separated on 12% sodium dodecyl sulfate-polyacrylamide gel electrophoresis (SDS-PAGE) and transferred to polyvinylidene fluoride (PVDF) membranes (Bio-Rad Laboratories GmbH) using a Trans-Blot Semi-Dry Transference apparatus (Bio-Rad Laboratories GmbH). Membranes were blocked with 5% BSA at room temperature for 2 h. Subsequently, they were incubated overnight at 4 °C with primary monoclonal anti-bodies: p53 (1:1000) and caspase-3 (1:1000). Antibodies against β-tubulin (1:5000) and GADPH (1:1000) were also used as internal standards. The membranes were incubated with anti-rabbit IgG (1:5000) or anti-mouse IgG (1:5000) at room temperature for 1 h and then detected with a chemiluminescent substrate (PierceTM ECL Western Blotting Substrate) and photographed

(Fujimedical Super RX-N, Fujifilm).

The relative densities of the protein bands were visualized and analyzed by Image Lab software (Bio-Rad, CA, USA) and NIH ImageJ software (Bethesda), respectively. The results represent the mean ± standard error of the mean (s.e.m.) of at least 2 experiments. Data were analyzed via one-way analysis of variance (ANOVA) followed by Dunnett's multiple comparisons test (GraphPad Prism v.6).

2.4.5. Morphological analysis

Cells were cultured in FluoroDish™ with cover glass bottom poly-D-lysine coated (World Precision Instruments Inc) at a density of 5×10^3 cells/plate. After 24 h incubation, U87-MG and U373-MG cells were treated with **1** and **4** respectively (10 μM), whereas SH-SY5Y cells were treated with **3** (1.77 μM) and further incubated for 24 h. DMSO (0.5%) treated cells were used as control. After that, they were washed with PBS and fixed with 4% neutral buffered formalin for 15 min at 4 °C.

DAPI (1 μg/mL) was added and cells were stained for 20 min at room temperature. Finally, cells were washed with PBS and observed in a Wide field microscope (Olympus IX51) using a cellSens Standard 4.1 software.

3. Results and discussion

Two new Schiff bases derived from the condensation reaction between a tosylsulfonamide amine and salicylaldehyde with one or two *tert*-butyl substituents, as ligands, were synthesized in good yields, and the isolated solids were characterized by elemental analysis, IR and ^{1}H NMR spectroscopy and mass spectrometry. Crystals of H_2L^1 and H_2L^2 suitable for X-ray studies were obtained (Fig. 1) by crystallization of the initial solid from methanol.

A series of new metal complexes were obtained by electrochemical synthesis with copper acting as the anode of an electrolytic cell containing the appropriate ligand. Heteroleptic complexes with 2,2′-bipyridine (2,2′-bpy), 4,4′-bipyridine (4,4′-bpy) or 1,10-phenanthroline (phen) as co-ligands were also obtained by addition of the corresponding coligand into the cell. In all cases, the elemental analysis shows that the metal ions react with the ligand at a 1:1 M ratio to afford complexes of the bi-deprotonated ligand (L^{2-}).

The electrochemical efficiency, E_f, defined as the amount of metal dissolved per Faraday of charge, was calculated in all the electrochemical processes. In all cases, this value is close to 1.0 mol·F^{-1} (see Experimental). These data and the evolution of dihydrogen at the cathode are consistent with the following mechanism:

$$\text{Cathode}: H_2L + 2e^- \rightarrow L^{2-} + H_2(g)$$

$$\text{Anode}: 2Cu \rightarrow 2Cu^+ + 2e^-$$

The analytical data suggests that the final products are compounds in which the oxidation state for the copper atom is +2, so the explanation could be that the copper atom suffers oxidation in solution from the state +1 to +2 as soon as it is formed. Same mechanism involving the electrochemical oxidation of Cu to Cu^{1+} followed by a further oxidation of Cu^{1+} to Cu^{2+} was also postulated for other copper(II) complexes obtained by electrochemical oxidation of copper anodes [34–35].

The final reaction can be represented by:

$$Cu + H_2L \rightarrow [CuL] + H_2(g)$$

or

$$Cu + H_2L + n\,L' \rightarrow \left[CuL(L')_n\right] + H_2(g)$$

where $n = 1$, L' = 2,2′-bpy or phen; n = 1/2 L' = 4,4′-bpy.

These complexes were characterized in the solid state using analytical and spectroscopic techniques. Results obtained from elemental analysis, UV–vis electronic absorption, FTIR are in good agreement with proposed formulations indicated in the experimental section.

3.1. Spectroscopic properties

The assignments of the main FTIR bands were made based in our previous reports of other copper(II) Schiff bases complexes [35]. The IR spectra do not show the bands attributed to ν(O—H) and ν(N—H), which appear near 3500 and 3250 cm^{-1} respectively for both free ligands. Also, the spectra of the complexes display the presence of the strong imine stretching band ν(C=N) in the range 1620–1605 cm^{-1} as predicted in the literature for the coordination of a Schiff base to a metal ion, and slightly shifted respect the position in the free ligands. In addition, the band attributed to ν(C—O) which appears at 1283 cm^{-1} in H_2L^1 and 1271 cm^{-1} in H_2L^2 appears shifted towards higher wavenumbers (1310–1295 cm^{-1}), approximately in all the complexes, and two strong bands in the ranges of 1385–1360 cm^{-1} and 1165–1175 cm^{-1} that are slightly shifted respect to the free ligand are assigned to ν_{as}(S=O) and ν_s(S=O) vibrations of the sulfonamide group. All these facts show indication of deprotonation of phenolic and sulfonamide protons during the electrochemical procedure, and that the ligand is in its dianionic form coordinated to the copper ion in the complexes.

The IR spectra of the heteroleptic complexes present additional

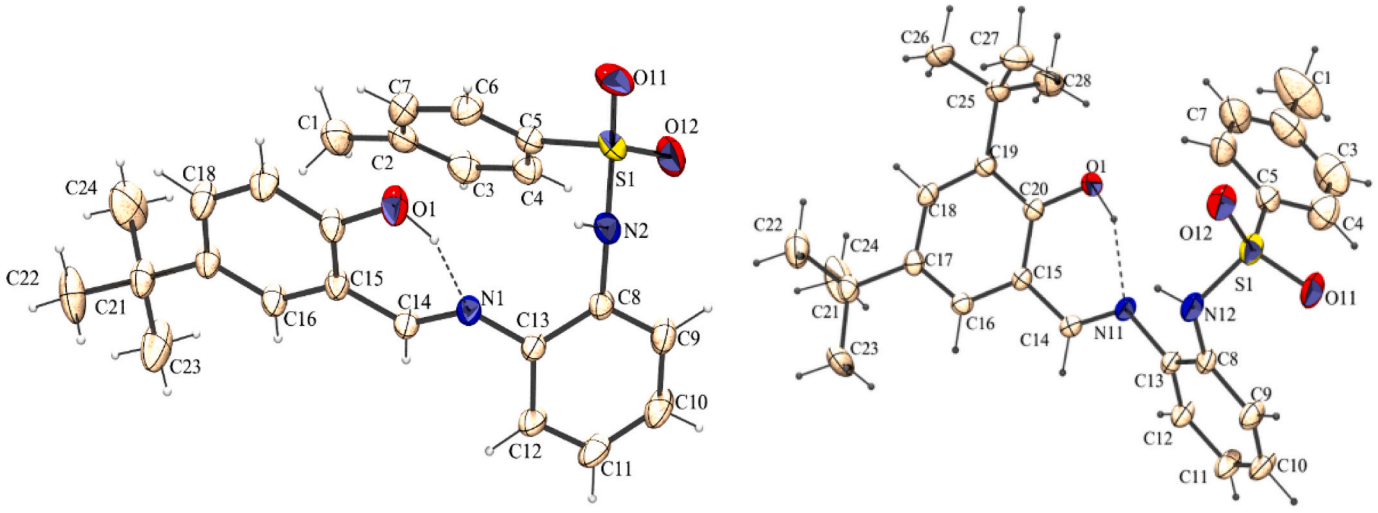

Fig. 1. Structures for the ligands H_2L^1 and H_2L^2, synthesized in this work. Displacements ellipsoids are drawn at the 30% probability level.

bands typical of coordinated 4,4-bpy [52] (1600, 1530 and 1000 cm^{-1}), 2,2′-bpy [53] (760 and 740 cm^{-1}) or 1,10-phenanthroline [53,54] (1510, 850 and 730 cm^{-1}).

The diffuse reflectance spectra of the [$CuL^1(H_2O)$], **(1)**; [$Cu_2L^1_2$(4,4′-bpy)] **(4)**; [$CuL^2(CH_3OH)$] **(5)** and [$Cu_2L^2_2$(4,4′-bpy)] **(8)** complexes show a broad band with a maximum at about 15000 cm^{-1}, which is in accordance with a square planar coordination around the copper(II) ion [35,55].

However, the spectra of [CuL^1(2,2′-bpy)]·(**2**)., [CuL^1(phen)] (H_2O) (**3**), [CuL^2(2,2′-bpy)] (**6**), and [CuL^2(phen)] (**7**) present a very broad band near to 10000 cm^{-1} and another at about 14500 cm^{-1}, which are typical for pentacoordinated d^9 systems with a distorted square pyramidal stereochemistry, in line with the X-ray structures described below.

3.2. Crystal structures analyses of some compounds

The molecular structure of the ligand H_2L^1 and ligand H_2L^2 and several of their metal complexes was determined by single X-ray diffraction analysis. A brief description of their structures is given here. In the Supplementary Material a more detailed description is provided. Fig. 1 contains an ORTEP [56] representation of the triclinic isomer of the *N*-[(5-*tert*-butyl-2-hydroxyphenyl)methylidine]-*N*′-tosylbenzene-1,2-diamine ligand, referred as H_2L^1. It is worth noting that a *C*2/*c* monoclinic isomer was also crystallized and studied but not important differences are found between them. It was possible to model the important disorder in the *tert*-butyl group [57] found in the triclinic isomer, in such a way that the methyl groups are split over, at least, two sites, with occupancy factors of 0.504(7):0.496(7). Even the most important intermolecular interaction, a hydrogen bond between the sulfonamide nitrogen atom and the phenolic oxygen atom of a neighbor molecule is also found in the monoclinic isomer.

Fig. 1 also contains a drawing of only one of the molecules found in the asymmetric unit for the compound *N*-[(3,5-di-*tert*-butyl-2-hydroxyphenyl)methylidine]-*N*′-tosylbenzene-1,2-diamine, [H_2L^2]. The most important bond lengths and angle are showed in Table S2 in Suppl. Mat. and compared with those of H_2L^1. Once more it was possible to model the important disorder found in one of the *tert*-butyl groups, with relative occupancy factors of 0.73(3):0.27(3), and it is possibly this disorder the reason of the existence of two molecules in the asymmetric unit, otherwise, there would be relation by a symmetry center in the middle of the $S_2O_2N_2H_2$ cycle. [58].

It should be noted that the hydrogen atoms bonded to the nitrogen or oxygen atoms were found in all cases in the final density map (see Experimental part) and their positions, together with other parameters found in the molecule corresponds with the imine-enolic form. [59] For example, N(1)-C(14) bond length, between 1.284(2) and 1.275(3) Å corresponds with a double bond, whereas O(1)-C(20) bond length, between 1.365(2) and 1.350(4) Å is an expected value for a phenolic C—O bond (about 1.36 Å) [60]. All other distances and angles are as expected. For the scope of this paper, the spatial disposition for the molecules is quite important, but in order to no enlarger this part, this discussion can be found in the Supplementary Material available. This material also contain a detailed study of the intermolecular interactions, studied under the point of view of the Hirshfeld surface analysis [61,62] and also from a crystallographic one (PLATON) [63].

We were also able to crystallize and study by means of x-ray diffraction some of the complexes synthesized with these ligands. In the following, the most interesting features of these structures, along a drawing of each one can be found, but the Suppl. Mat. contains an exhaustive discussion of the spatial disposition together a detailed study of their intermolecular interactions and a selection of bond distances and angles. This series of description begins with the simplest [CuL^2(-MeOH)] compound where the metal atom completes the coordination environment with a solvent molecule. Following there are the study of the complexes with formula [CuLL'], where the tridentate Schiff base (L) and an additional bidentate ligand (2,2′-bpy or 1,10-phen) is offered to the metal in order to fulfill a five-coordination number. Finally, an additional but no-chelating bidentate ligand (4,4′-bpy) was included in the reaction to generate dinuclear complexes.

Fig. 2 displays an ORTEP [56] drawing of [CuL^2(MeOH)] showing the numbering scheme used. For all the complexes crystallographically described in this paper, the numbering scheme for the Schiff base is the same used in the free ligand (see above). In [CuL^2(MeOH)] the copper (II) atom is four-coordinated by two nitrogen atoms and one oxygen atom of the tridentate Schiff base ligand, and another oxygen atom of a coordinated neutral methanol molecule, forming a distorted square-planar coordination configuration. A τ_4 parameter of 0.12 allows us to define the environment of the metal atom as a slightly distorted square plane [64].The Cu—O and the Cu—N bond distances are only slightly longer than those found in other methanolic copper(II) complexes with tridentate Schiff bases [65,66], or in other tetracoordinated Schiff bases copper complexes [67]. Four-fused ring (1 to 4 in Figure) are found in the structure, the aminophenolate moiety benzene ring, a six-membered metallacycle, a five-membered metallacycle, and the diaminebenzene moiety benzene ring. These are twisted in such a way that the dihedral angles between fused rings are, in the same order (left to right in Fig. 2) are 4.3(2), 14.1(2) and 11.0(3)°, with an overall result of a dihedral angle between both benzene rings of 23.4(3)°. Of course the tolyl ring is out of this plane, almost perpendicular, and it is forming a dihedral angle with the diaminebenzene moiety benzene ring of 75.7(3)°. This disposition allows a π,π-stacking of the molecules in the supramolecular plane.

Figs. 3, 4 and 5 display an ORTEP [56] drawing of the compounds [CuL^1(2,2′-bpy)] **(2)**, [CuL^2(2,2′-bpy)] **(6)** and of [CuL^2(1,10-phen)] **(7)**. The structure of these complexes consists in discrete monomer units, in which the copper atom is pentacoordinated by the imino and amidate nitrogen atoms and the phenolate oxygen of the corresponding tridentate dianionic Schiff base ligand and the two nitrogen atoms from the 2,2′-bipyridine or from the 1,10-phenanthroline molecule, respectively. The coordination environment around the metal atom better defined as a distorted square pyramid (τ_5 = 0.29, 0.10 or 0.01, respectively) [68] with one of the nitrogen atoms of the 2,2′-bipyridine or the 1,10-phenanthroline molecule occupying the apical position. Geometrical parameters as bond distances and angles are as expected and do not deserve more comments here. As in previous complex described, four fused ring are found in the structure, once more labelled consecutively as 1 to 4 in Scheme 2. These are twisted in such a way that the dihedral angles between fused rings are, in the same order 3.2(1), 20.31(8) and 14.10 (10)° with an overall result of a dihedral angle between both benzene rings [dihedral angle between 1 and 4] of 22.51(11)° for [CuL^1(2,2′-bpy)] **(2)**, 6.7(2), 11.8(2), 5.4(3)° and 20.0(3)° for [CuL^2(2,2′-bpy)] **(6)** and in the case of [CuL^2(1,10-phen)] **(7)** those values are, respectively 6.04(10), 8.33(9) and 2.40(12)°, and an overall value of 9.73(13)°. It is worthy than the Schiff base ligand is much more planar than it is in [CuL^2(MeOH)] **(5)** compound (see above), and more planar in the phen compound than in the bpy compounds. The plane formed by the neutral ligand is situated almost perpendicular to the basal plane, with a dihedral angle of 77.62(6), 87.9(1)° and 86.02(4)°, respectively.

Fig. 6 displays an ORTEP [56] drawing of the compound [$Cu_2L^1_2$(4,4′-bpy)] (**4**). The complex is composed of dinuclear units, where one half is of the molecule is in the asymmetric unit. The other half is symmetry generated (1-x, 1-y, −z) so there is only one half of the 4,4′-bpy ligand in the asymmetric unit together with the metal atoms and the dianionic tridentated Schiff base ligand. Once more this ligand bonded the metal by using the imino nitrogen atom, the phenolate oxygen atom and the amidate nitrogen atom. The coordination polyhedron around the both copper atoms are identical (symmetry imposed) and is best described as a square planar, although highly distorted, since the atom sulfonamide nitrogen atom N(2) is clearly deviated from the best plane, with root-mean-square (rms) deviation from the best plane of 0.2644 Å. Noteworthy the tolyl substituent almost parallel to the plane of the rest of Schiff base molecule, and the N(2)-S(1) bond form an angle of 47.55(8)

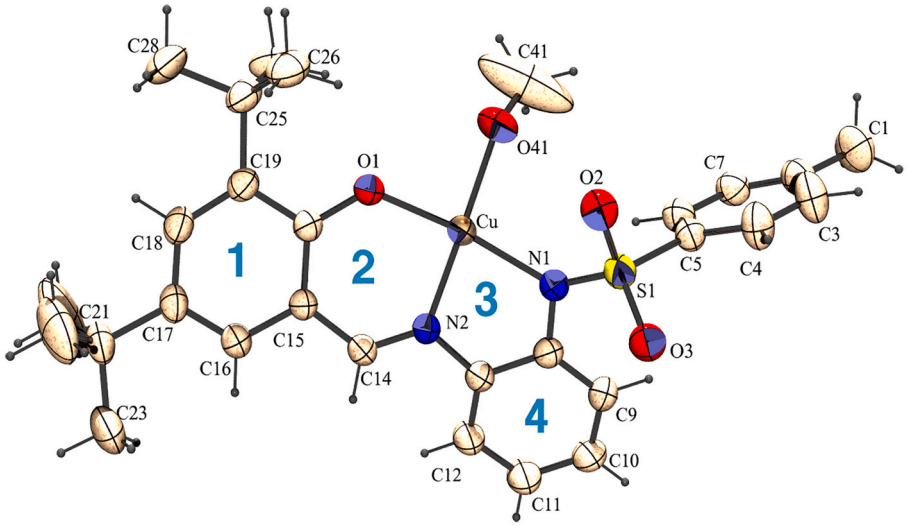

Fig. 2. Ortep drawn at 30% probability level of [CuL^2(MeOH)] Hydrogen atoms as spheres of arbitrary radius. Numbers identify cycles, see text.

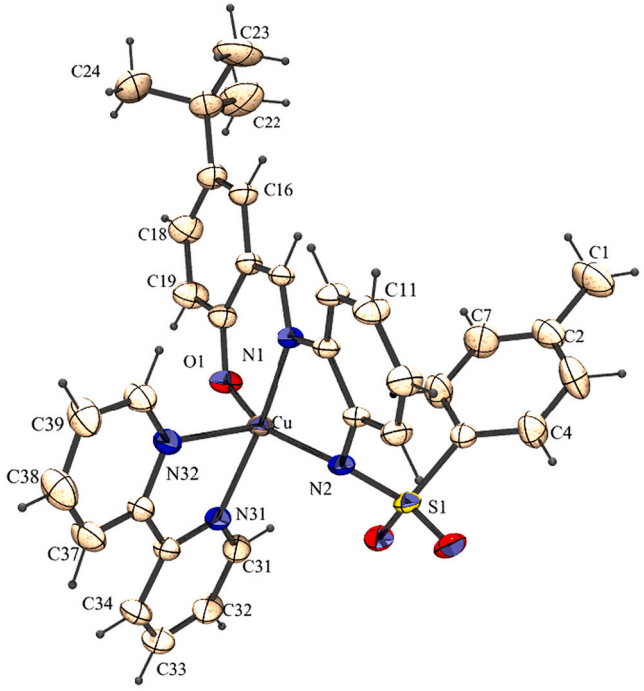

Fig. 3. ORTEP drawing of [CuL^1(2,2′-bpy)].

with the 5-membered metallacycle found in the complex.

The bond lengths between the copper atom and the Schiff base donor atoms (See Table S11) are Cu-O(1), 1.887(3); Cu-N(1), 1.938(3); Cu-N (2); 2.006(3) and Cu-N(31), 2.007(3) Å are similar to those found in other square planar copper(II) complexes [69] and do not deserve more comments. In the Supplementary Material a detailed description and a study of the supramolecular arrangement can be found.

3.3. Hirshfeld surface

Hirshfeld surface analysis allows the vision of all interactions in crystal structures [61]. This method uses visual recognition of properties of intermolecular interactions through mapping onto this surface. Generated figures show colored regions, red ones indicate contacts shorter than the sum of the van der Waals radii, and blue ones indicate contacts shorter and white ones represent the contacts closer to the van der Waals radii. In addition, all (d_i, d_e) contacts can be expressed in the form of a two dimensional plot, known as the 2D fingerprint plot. These could be separated in such a way that the contributions of individual interactions could be plotted with the percentage of each contribution. These were calculated as reciprocal, that is, they contain the X…Y and the Y…X interaction in the same plot. The d_i and d_e are defined, respectively, as the distance from the Hirshfeld surface to the nearest nucleus outwards from the surface and the distance from the surface to the nearest atom in the molecule itself. The shape of this plot, which is unique for each molecule, is determined by dominating intermolecular contacts. The Hirshfeld surface was calculated using the Crystal Explorer v.3.1 program package and the 2D fingerprint was prepared using the same software [62].

Results for these studies are set out in the supplementary material. As an example, Fig. 7 shows the Hirshfeld surface analysis under d_{norm}. For H_2L^2, and Fig. 8 the corresponding 2D fingerprints for its intramolecular interactions. In the case of the free ligand, the interactions are mainly driven by van der Waals forces (H···H contacts, between 56.2 and 67.5%, see Figs. 8 and S9) but the shorter ones, and consequently the source of the red spots in these graphics are the O…H interactions (contribution between 11.4% for H_2L^2 or 21.7% for the monoclinic form of H_2L^1). These are show in the corresponding 2D fingerprints as two acute spikes beginning below 2 Å ($d_i + d_e$), and a red spots in the left of Fig. 7, where a N-H…O is remarked.

For the complexes, the situation is quite different. For example, in the case of [CuL^2(MeOH)], see Fig. S15, besides of the van der Waals forces (H···H contacts, begin at <1.9 Å), a Cu…O interaction (about $d_i + d_e$ of 2.8 Å) is found as a characteristic red spot in the Hirshfeld surface plot, and two acute spikes in the corresponding 2D fingerprint (of course, shadowed for other interactions). In the other complexes, the Cu…O is not so important than the C…H interaction, due the mentioned π,π-stacking found, especially in the 1,10-phenantroline complex.

3.4. Biological studies

3.4.1. Anti-proliferative activity of the copper(II) complexes against cancer cells

Toxicity of different concentrations of copper(II) complexes **1**–**8** (0.5–50 μM) was studied in three cancer SH-SY5Y, U87-MG and U373-MG cell lines. As shown in Table 1, all molecules displayed toxicity towards the three cell lines. In general, the copper(II) complexes **(1–8)** showed greater toxicity on SH-SY5Y line than on glioblastoma lines (U87-MG and U373-MG). Copper complexes with the dianionic ligand

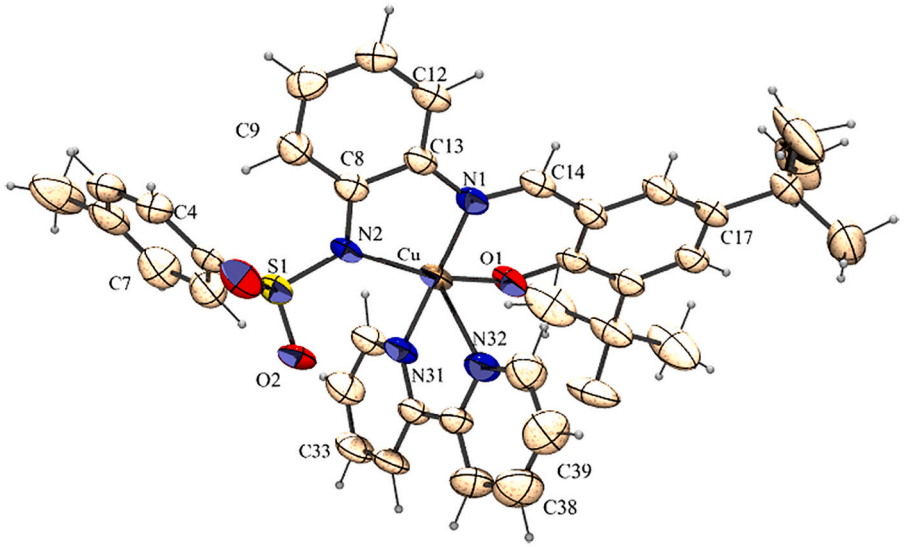

Fig. 4. ORTEP drawing of [CuL^2(2,2′-bpy)].

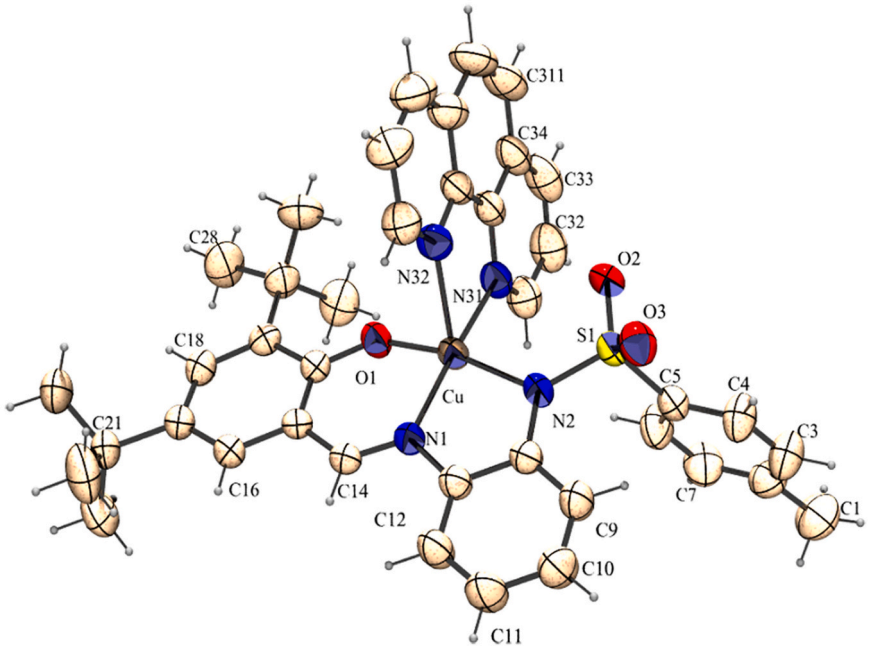

Fig. 5. ORTEP drawing of [CuL^2(1,10-phen)].

L^1 (**1**–**4**) resulted most potent on the SH-SY5Y cell line, with IC_{50} of 1.77 μM for compound **3**. Copper(II) complex **4** resulted the most potent on U87-MG and U373-MG with IC_{50} of 11.83 μM and 12.92 μM respectively. All three lines were shown to be more susceptible to the studied copper(II) complexes (**1–8**) than to cisplatin. Our results are in agreement with those previously described by other authors. Stefani et al. (2015) described the antiproliferative activity of a series of copper complexes with Schiff bases on the SK-N_MC cell line, a precursor of SH-SY5Y line [70]. Although the effects of this type of complex on glioblastoma lines are less studied, Konarikova et al. demonstrated an antiproliferative effect on the U118-MG line through enzymatic inactivation of the Pi3K/Akt/mTOR pathway [71].

Copper(II) complexes **1**, **3** and **4** were selected for further studies. They showed a lower toxicity in MRC-5 cell line than in the corresponding cancer cell lines used in this study.

3.4.2. Impact of the copper(II) complexes upon intracellular ROS levels

To determine the mechanisms underlying cell death induced by copper complexes **1**, **3** and **4**, we evaluated the ability of these compounds to induce oxidative stress. Since ROS is an important indicator of oxidative stress and cell injury, the ROS levels in the three cell lines treated with these compounds were evaluated. The results indicated that, compared to the control group, the ROS production levels were significantly increased after treatment of SH-SY5Y cell line with **3**. This result is in agreement with Filomeni et al. who also described stress oxidative produced by treatment with bis[(2-oxindol-3-ylimino)-2-(2-aminoethyl)pyridine-*N,N′*]copper(II) complex in SH-SY5Y cells [72] (Fig. 9).

Increase in ROS levels has been also associated to glioblastoma cell toxicity [73]. However, in contrast to the above results described for SH-SY5Y cells, treatment of U87-MG cells with compounds **1** did not significatively modify ROS production whereas compound **4** significantly

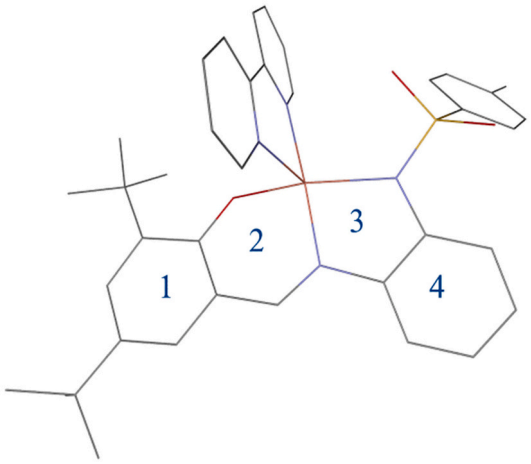

Scheme 2. Numbering for the four-fused rings system.

reduced ROS production in U373-MG cells at higher concentrations (Fig. 9), ruling out ROS production involvement in cell death.

3.4.3. *Modulation of caspase 3 and p53 expression and cell death by copper(II) complexes*

Analysis of the proteins expression that trigger cell apoptosis was performed by western blot. Caspase-3 becomes activated during apoptosis and can therefore be used as an apoptotic marker as can caspase-9, which is located upstream of caspase-3. Previous studies with copper(II) complexes with Schiff base ligands in colon cancer cells, showed an intrinsic apoptotic pathway with a high activation of caspase-3 mediated by the production of ROS [74]. In SH-SY5Y it has been described that ROS production induces apoptotic cell death via activation of caspase-9 and caspase-3 through activation of MAPK pathways [75]. Therefore, we studied expression of caspase-3 in SHSY5Y cells treated with compound **3** at concentration 1.77 μM that significantly increased ROS production. Contrary to expectations, this treatment did not modify caspase-3 gene expression. Neither did the treatment of U87-MG with compound **1** or U373-MG with compound **4** modify the expression of caspase-3 in these cell lines (Fig. 10).

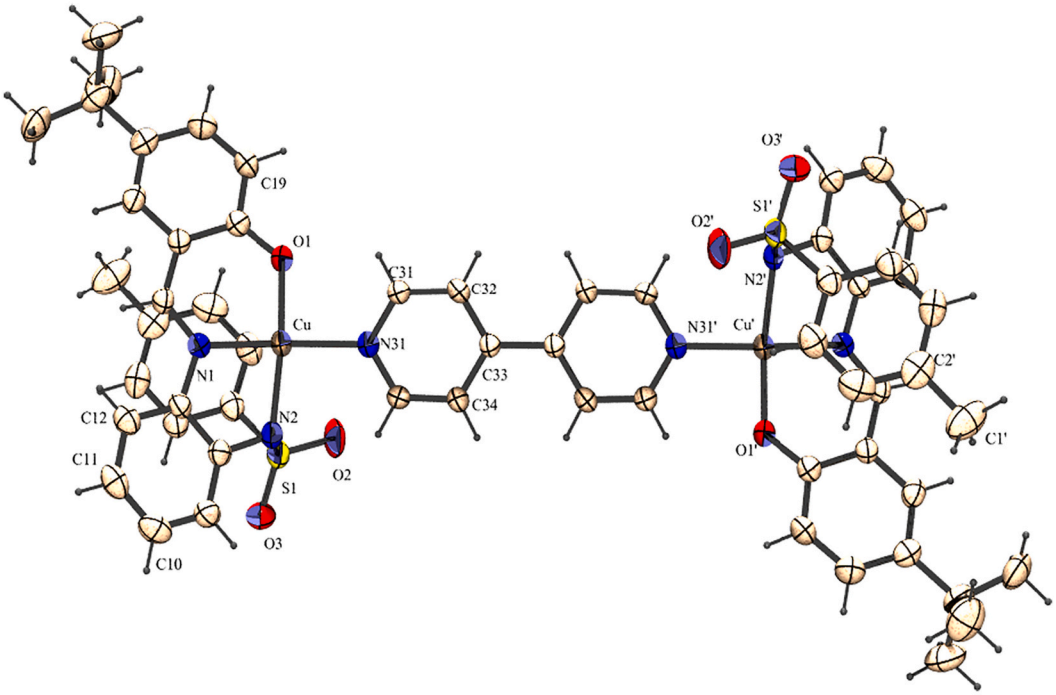

Fig. 6. ORTEP drawing of $[Cu_2L^1_2(4,4'\text{-bpy})]$ (**4**).

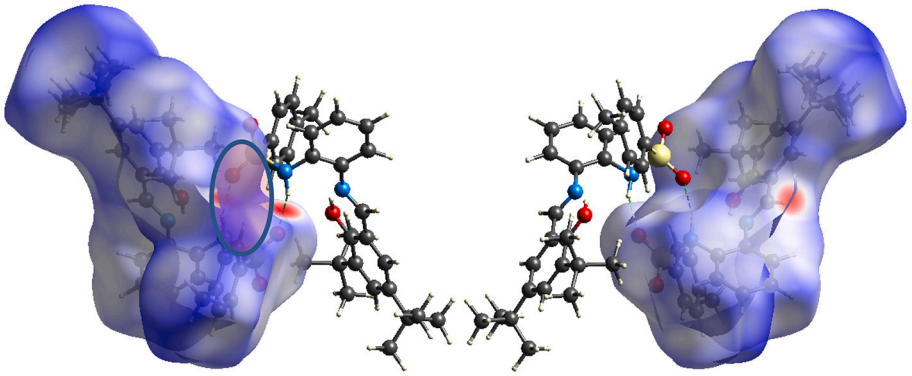

Fig. 7. Opposite (180° roted) views of the Hirshfeld surface for H_2L^2 mapped with d_{norm} function.

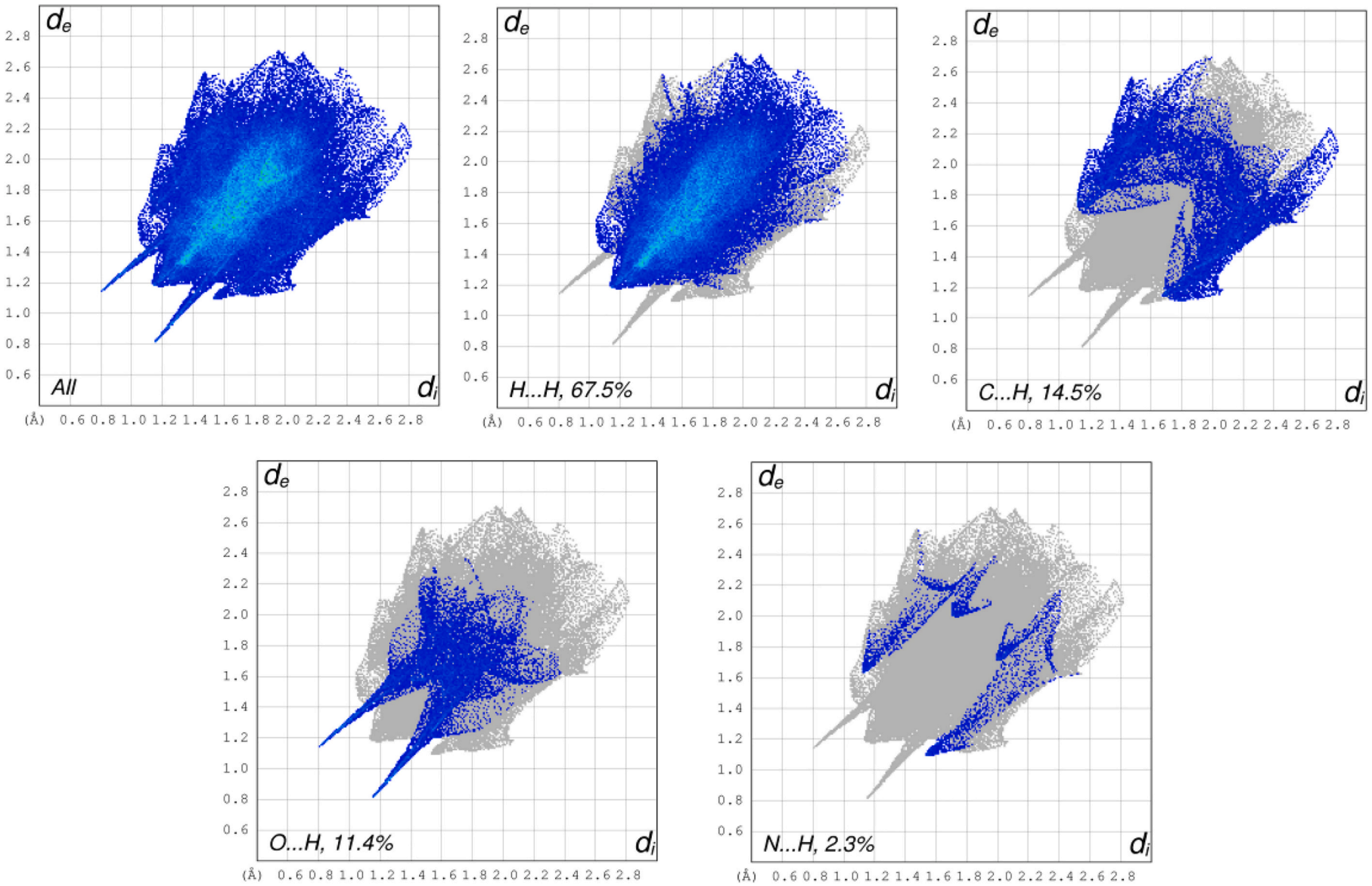

Fig. 8. 2D fingerprints for H_2L^2. Reciprocal contributions are included.

Table 1
Cytotoxicity (IC_{50}, μM) of ligands and copper(II) complexes towards the SH-SY5Y, U87-MG, U373-MG and MRC-5 cell lines, as evaluated by the MTT assay.

Compound	IC_{50} (μM)						
	SH-SY5Y	U87-MG	U373-MG	MRC-5	SI SH-SY5Y	SI U87-MG	SI U373-MG
H_2L^1	> 50	> 50	> 50	–	–	–	–
H_2L^2	21.69 ± 3.25	> 50	> 50	–	–	–	–
$[CuL^1(H_2O)]$ **(1)**	2.81 ± 0.42	16.14 ± 1.08	16.92 ± 1.13	19.08 ± 0.48	6.8	1.2	1.1
$[CuL^1(2,2\text{-bpy})]$ **(2)**	2.63 ± 0.40	20.09 ± 0.05	14.42 ± 0.96	16.85 ± 0.57	6.4	0.8	1.2
$[CuL^1(phen)]$ **(3)**	1.77 ± 0.27	22.19 ± 1.48	16.03 ± 1.33	18.20 ± 0.33	10.2	0.8	1.1
$[Cu_2L^1_2(4,4'\text{-bpy})]$ **(4)**	2.85 ± 0.43	11.83 ± 1.07	12.92 ± 1.05	19.94 ± 1.72	7.0	1.7	1.5
$[CuL^2(MeOH)]$ **(5)**	9.06 ± 1.36	26.73 ± 5.26	17.61 ± 2.27	25.39 ± 1.32	2.8	0.9	1.4
$[CuL^2(2,2\text{-bpy})]$ **(6)**	23.55 ± 3.53	22.25 ± 0.89	19.78 ± 2.03	24.91 ± 1.26	1.1	1.1	1.3
$[CuL^2(phen)]$ **(7)**	5.57 ± 0.84	25.92 ± 1.25	22.52 ± 1.35	24.92 ± 2.28	4.7	1.0	1.1
$[Cu_2L^2_2(4,4'\text{-bpy})]$ **(8)**	21.43 ± 3.22	> 50	23.71 ± 1.37	20.34 ± 0.20	0.9	< 0.5	0.9
Cisplatin	27.50 ± 4.30	> 100	~150	–	–	–	–

Each value represents the mean ± s.e.m. from at least 5 experiments. The IC_{50} ± s.e.m. values given in micromolar concentrations were obtained using dose-response curve by nonlinear regression using GraphPad prism version 5.0. SI: Selectivity index calculated as IC_{50} MRC-5/IC_{50} tumor cell line.

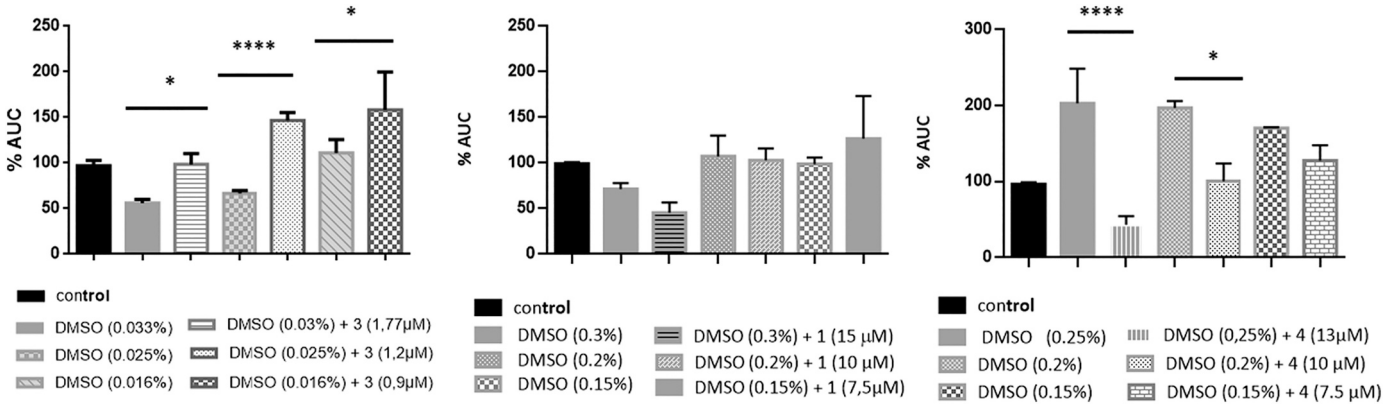

Fig. 9. Effects of different concentrations of vehicle (DMSO) and compounds **3**, **1** and **4** on ROS production in SH-SY5Y, U87-MG and U373-MG cell lines respectively after 24 h treatment. Every bar represents the mean ± s.e.m. of three independent experiments. *$p < 0.05$ and ****$p < 0.0001$ versus cells treated with DMSO.

In previous works, Filomeni et al. identified AMPK/p38MAPK induction as the cell death signaling pathway activated as a consequence of oxidative stress induced by the complex bis[(2-oxindol-3-ylimino)-2-(2-aminoethyl)pyridine-*N,N′*]copper(II) in SH-SY5Y cells. Apoptosis is ultimately mediated by p53 [72]. p53 is usually present at low levels in the cell due to its short half-life but it accumulates by mutation. However, in neuroblastoma cells, p53 is not mutated but high levels of wild-type (wt) p53 protein are retained in the cytoplasm of undifferentiated cells and it is also accumulated in the nucleus as an inactive conformation [76]. As expected, p53 protein extracted from SH-SY5Y migrated at the wt position (Fig. 11). Of particular note is an additional faint band that migrated faster than the full-length protein. This

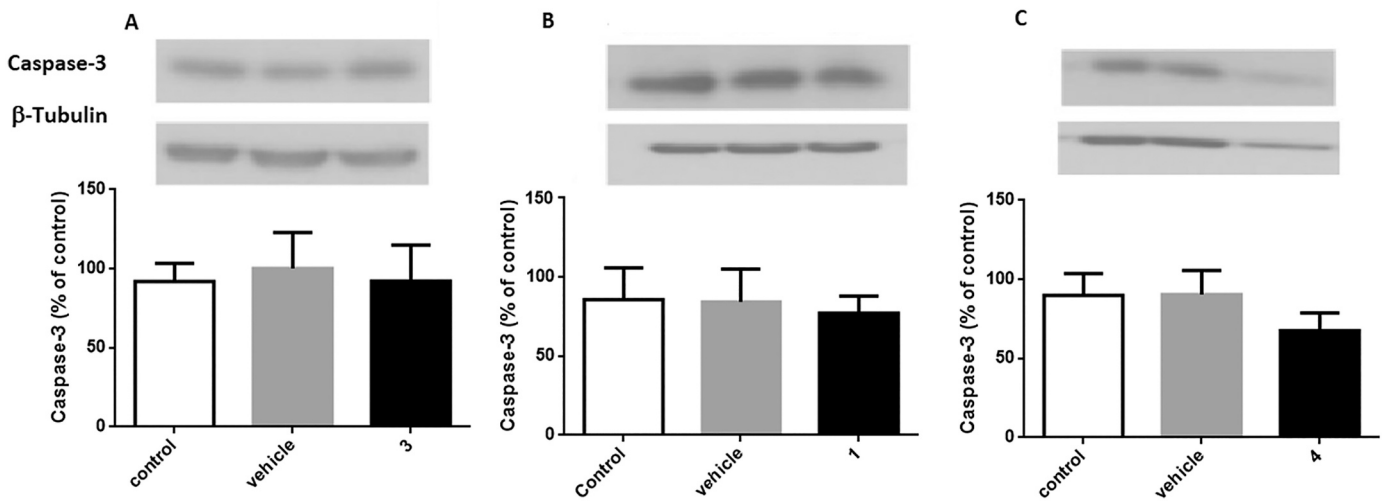

Fig. 10. Changes in caspase-3 expression in tumoral cell lines. (A) SH-SY5Y cells treated with vehicle (DMSO, 0.03%) or copper(II) complex **3** (1.77 μM). (B) U87-MG cells treated with vehicle (DMSO, 0.2%) or **1** (10 μM). (C) U373-MG cells treated with vehicle (DMSO, 0.2%) or **4** (10 μM). Every bar represents the mean ± s.e.m. of at least, two independent experiments.

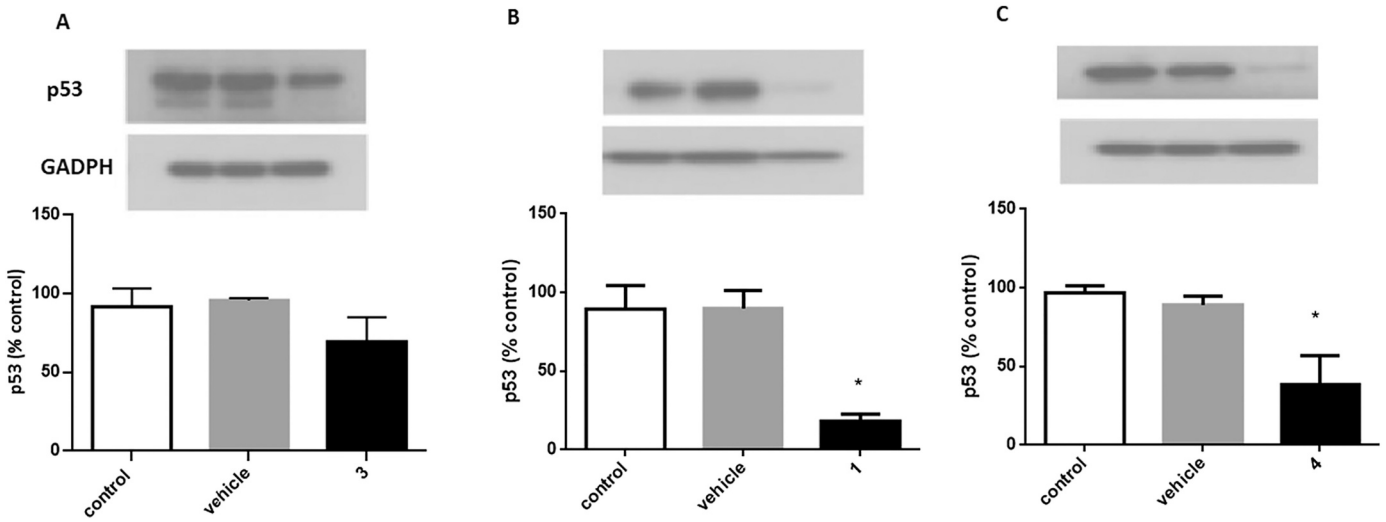

Fig. 11. Changes in p53 expression in tumoral cell lines. (A) SH-SY5Y cells treated with vehicle (DMSO, 0.03%) or copper(II) complex **3** (1.77 μM). (B) U87-MG cells treated with vehicle (DMSO, 0.2%) or **1** (10 μM). (C) U373-MG cells treated with vehicle (DMSO, 0.2%) or **4** (10 μM). Every bar represents the mean ± s.e.m. of at least, two independent experiments. $^{*}p < 0.05$.

band was previously identified in SH-SY5Y cell line by Goldschneider et al. as the β isoform [77]. p53β can induce apoptosis independently of p53, but to a lesser extent than p53. p53β in combination with p53 induces senescence and enhances p53-mediated apoptosis [78]. Compound **3** inhibited p53β expression, however it did not significantly modify p53 expression level (Fig. 11). Further studies would be necessary to clarify if compound **3** modifies subcellular localization of p53 in the cytoplasm and nucleus of SH-SY5Y cells.

In U87-MG cells, p53 exists in a non-mutated form and has been involved in the response of these cells to anti-cancer compounds whereas U373-MG contains mutant p53 alleles [79]. Treatment of U373-MG with compound **4** or U87-MG with **1** significantly decreased expression of p53 in these cell lines (Fig. 11). It has been described in other cell models as limb cells than absence of p53 may decreases DNA repair capacity and contribute to the accumulation of DNA damage. The failure of apoptosis to eliminate cells with DNA damage may result in increases cell death by necrosis [80].

The results obtained indicate that these copper(II) complexes do not seem to induce cell death by increasing the expression of genes related to apoptosis.

It also has been described that gene knock-out of p53 can induce autophagy. However, it occurs in the G1 and at lower extent in the S phase, but not in the G2/M phase of the cell cycle [81]. Therefore, further studies are necessary in order to determine the exact mechanisms by which these copper complexes cause cell death.

3.4.4. Morphological changes induced by copper(II) complexes and cell death

To better understand the different cytotoxic effects of compounds **1**, **3** and **4** on neuroblastoma cell line SH-SY5Y and glioblastoma cell lines U87-MG and U373-MG we performed representative photographs at light microscope of treated cells for 24 h with DMSO (Control) and compounds **1**, **3** and **4**. Additionally, DAPI staining was performed to ascertain cell death mechanism and the degree of cellular damage.

After 24 h treatment of SHSY5Y cells with copper complex **3** and U87-MG and U373-MG cells with copper complex **1** and **4** respectively, led to rounding of cells and slight membrane disruption compared to control cells treated with vehicle (Fig. 12). In U87-MG and U373-MG cells, DAPI staining of the nucleus revealed changes in chromatin shape and condensation after treatment with complexes **1** and **4** respectively. In SH-SY5Y cells the nuclei remain intact after complex **3** treatment (Fig. 13). Chromatin condensation is also not observed. The

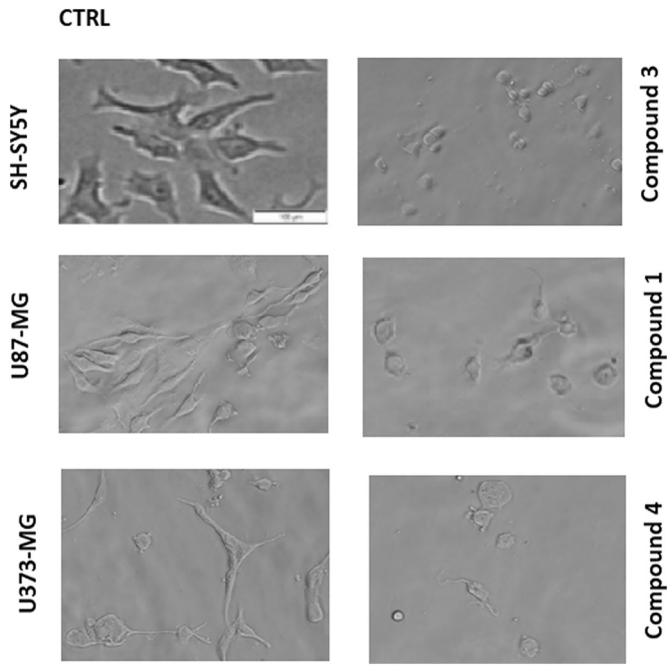

Fig. 12. Morphological images of the three cell lines: SH-SY5Y, U87-MG and U373-MG. Representative cells images at light microscope: control cells treated with vehicle DMSO 0.5% (CTRL) and cells treated 24 h with copper(II) complexes **3** (1.77 μM), **1** and **4** (10 μM) respectively. (Magnification 40×).

non-alteration of the nuclei together with the increase in ROS production could suggest cell death by necroptosis. Recently, accumulating evidence shows that various compounds can exhibit the anti-cancer effect via inducing regulated necrosis in cancer cells, which indicates that caspase-independent regulated necrosis pathways are potential targets in cancer management [82].

4. Conclusions

Two new potentially tridentated Schiff base ligands were design and synthetized. A number of copper(II) complexes of these ligands were prepared by following an electrochemical procedure, allowing, in a one

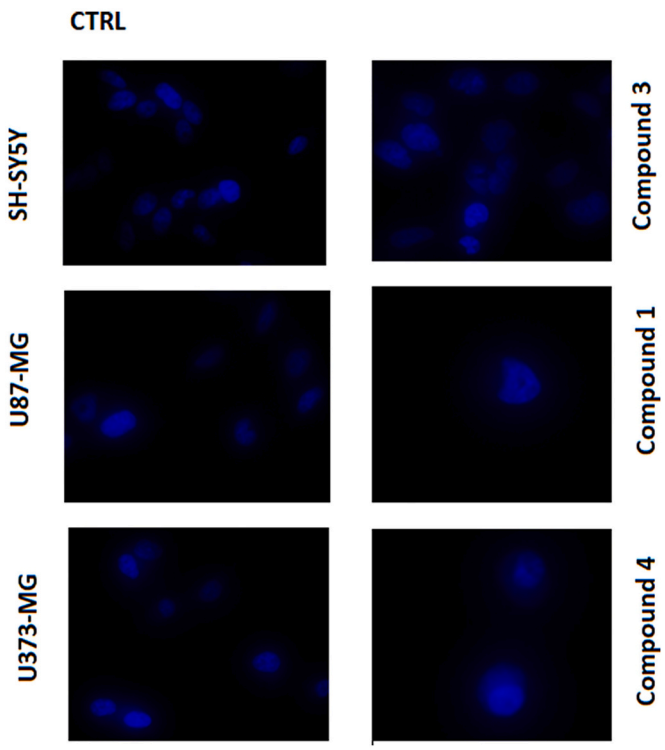

Fig. 13. Evaluation of chromatin status by using DAPI. Representative fluorescence images of control cells treated with DMSO 0.5% (CTRL) and cells treated 24 h with copper(II) complexes **3** (1.77 μM), **1** and **4** (10 μM) respectively. (Magnification 40×).

pot reaction to obtain several complexes on depending of the electrochemical cell containing. If only the Schiff base is present, solvent is used to complete the environment of copper atom up to tetra-coordination. When additional chelating ligand is provided, pentacoordinated complexes were obtained. If additional spacer ligand is provided, dinuclear compounds were synthetized. Ligands and complexes were characterized by means of representative spectroscopical methods, and at least for a representative example of each type, a crystallographic study was performed and the molecular and supramolecular structure discussed.

The antitumor activity of this new series of compounds was investigated against SH-SY5Y neuroblastoma cell line and U87-MG and U373-MG glioblastoma cell lines. Most of the test compounds showed higher activity that cisplatin in all tumoral cell lines studied. In general, the copper(II) complexes that present the dianionic form of ligand L^1 resulted to be more cytotoxic in the different tumor cell lines.

Preliminary results seem to indicate that compound **3** could cause necroptosis in SH-SY5Y cells while **1** and **4** could cause necrosis in U87-MG and U373-MG cells, respectively. Further studies are necessary to better clarification of mechanism of action.

CRediT authorship contribution statement

María Diz: Investigation. **María L. Durán-Carril:** Validation, Writing – original draft. **Jesús Castro:** Conceptualization, Formal analysis, Supervision, Writing – original draft. **Samuel Alvo:** Investigation. **Lucía Bada:** Investigation. **Dolores Viña:** Investigation, Validation, Writing – original draft. **José A. García-Vázquez:** Conceptualization, Formal analysis, Supervision, Writing – original draft.

Declaration of Competing Interest

The authors declare that they have no known competing financial interests or personal relationships that could have appeared to influence the work reported in this paper.

Data availability

No data was used for the research described in the article.

Acknowledge

This work has received financial support from the Xunta de Galicia (Centro de investigación de Galicia accreditation 2019–2022) and the European Union (European Regional Development Fund - ERDF).

Appendix A. Supplementary data

Supplementary data to this article can be found online at https://doi.org/10.1016/j.jinorgbio.2022.111975.

References

[1] F. Bray, J. Ferlay, I. Soerjomataram, R.L. Siegel, L.A. Torre, A. Jemal, CA Cancer J. Clin. 68 (2018) 394–424, https://doi.org/10.3322/caac.21492. Article corrected in 2020, Doi: 10.3322/caac.21609.
[2] The International Agency for Research on Cancer (IARC). https://gco.iarc.fr/tomorrow/en, 2022. Accessed June.
[3] K. Hu, F. Li, Z. Zhanga, F. Liang, New J. Chem. 41 (2017) 2062–2072, https://doi.org/10.1039/c6nj02483a.
[4] Y. Jung, S.J. Lippard, Chem. Rev. 107 (2007) 1387–1407, https://doi.org/10.1021/cr068207j.
[5] T.C. Johnstone, K. Suntharalingam, S.J. Lippard, Chem. Rev. 116 (2016) 3436–3486, https://doi.org/10.1021/acs.chemrev.5b00597.
[6] F. Trudu, F. Amato, P. Vaňhara, T. Pivetta, E.M. Peña-Méndez, J. Havel, J. Appl. Biomed. 13 (2015) 79–103, https://doi.org/10.1016/j.jab.2015.03.003.
[7] F. Arnesano, G. Natile, Coord. Chem. Rev. 253 (2009) 2070–2081, https://doi.org/10.1016/j.ccr.2009.01.028.
[8] N. Pabla, Z. Dong, Kidney Int. 73 (2008) 994–1007, https://doi.org/10.1038/sj.ki.5002786.
[9] B.J. Pages, K.B. Garbutcheon-Singh, J.R. Aldrich-Wright, Eur. J. Inorg. Chem. (2017) 1613–1624, https://doi.org/10.1002/ejic.201601204.
[10] M.G. Apps, E.H.Y. Choi, N.J. Wheate, Endocr. Relat. Cancer 22 (2015) R219–R233, https://doi.org/10.1530/ERC-15-0237.
[11] K. Hu, F. Li, Z. Zhanga, F. Liang, New J. Chem. 41 (2017) 2062–2072, https://doi.org/10.1039/c6nj02483a.
[12] E. Alessio, Z. Guo, Eur. J. Inorg. Chem. (2017) 1539–1540, https://doi.org/10.1002/ejic.201700196.
[13] A. Bergamoa, G. Sava, Chem. Soc. Rev. 44 (2015) 8818–8835, https://doi.org/10.1039/C5CS00134J.
[14] S. Medici, M. Peana, V.M. Nurchi, J.I. Lachowicz, G. Crisponi, M.A. Zoroddu, Coord. Chem. Rev. 284 (2015) 329–350, https://doi.org/10.1016/j.ccr.2014.08.002.
[15] S.P. Fricker, Dalton Trans. (2007) 4903–4917, https://doi.org/10.1039/b705551j. Y. Li, B. Liu, H. Shi, Y. Wang, Q. Sun, Q. Zhang Dalton Trans., 50, (2021), 14498-14512, Doi: 10.1039/d1dt02909f.
[16] M. Gielen, E.R.T. Tiekink, Metallotherapeutic Drugs and Metal-Based Diagnostic Agents: The Use of Metals in Medicine, Wiley, England, 2005, https://doi.org/10.1002/0470864052.
[17] I. Romero-Canelón, P.J. Sadler, Inorg. Chem. 52 (2013) 12276–12291, https://doi.org/10.1021/ic400835n. T. Tõpala, A. Pascual-Álvarez, M. A. Moldes-Tolosa, A. Bodoki, A. Castiñeiras, J. Torres, C. del Pozo, J. Borrás, G. Alzuet-Piña J. Inorg. Biochem. 202, (2020), 110823, Doi: 10.1016/j.jinorgbio.2019.110823.
[18] A.L. Lainé, C. Passirani, Curr. Opin. Pharmacol. 12 (2012) 420–426, https://doi.org/10.1016/j.coph.2012.04.006.
[19] a) P. Zhang, P.J. Sadler, Eur. J. Inorg. Chem (2017) 1541–1548, https://doi.org/10.1002/ejic.201600908;
b) J.C. Pessoa I, Correia Coord, Chem. Rev. 388 (2019) 227–247, https://doi.org/10.1016/j.ccr.2019.02.035;
H.K. Saeed S., Sreedharan, J. A Thomas Chem, Commun. 56 (2020) 1464–1480, https://doi.org/10.1039/c9cc09312e;
c)K. Kar, D. Ghosh, B. Kabi A, (2022). Chandra Polyhedron, 222. 115890-0, Doi: 10.1016/j.poly.2022.115890.
[20] J.C. García-Ramos, G. Vértiz-Serrano, L. Macías-Rosales, R. Galindo-Murillo, Y. Toledano-Magaña, J.P. Bernal, F. Cortés-Guzmán, L. Ruiz-Azuara, Eur. J. Inorg. Chem. (2017) 1728–1736, https://doi.org/10.1002/ejic.201601199.
[21] S.M.G. Leite, L.M.P. Lima, S. Gama, F. Mendes, M. Orio, I. Bento, A. Paulo, R. Delgado, O. Iranzo, Inorg. Chem. 55 (2016) 11801–11814, https://doi.org/10.1021/acs.inorgchem.6b01884.
[22] W.-J. Lian, X.-T. Wang, C.-Z. Xie, H. Tian, X.-Q. Song, H.-T. Pan, X. Qiao, J.-Y. Xu, Dalton Trans. 45 (2016) 9073–9087, https://doi.org/10.1039/c6dt00461j. P. Yang, D. D. Zhang, Z. Z. Wang, H.Z. Liu, Q. S. Shi, X.B. Xie Dalton Trans., 48, (2019), 17925–17935 Doi: 10.1039/c9dt03746b.

[23] J. Qi, Y. Zhang, Y. Gou, Z. Zhang, Z. Zhou, X. Wu, F. Yang, H. Liang, Mol. Pharm. 13 (2016) 1501–1507, https://doi.org/10.1021/acs.molpharmaceut.5b00938.

[24] D. Denoyer, S. Masaldan, S. La Fontaine, M.A. Cater, Metallomics 7 (2015) 1459–1476, https://doi.org/10.1039/c5mt00149h.

[25] C. Wende, C. Lüdtke, N. Kulak, Eur. J. Inorg. Chem. (2014) 2597–2612, https://doi.org/10.1002/ejic.201400032. N. Mohan, C. V. Vidhya, V. Suni, J. M. Ameer, N. Kasoju, P. V. Mohanan, S. S. Sreejith, M. R. P. Kurup *New J. Chem.*, 46, **(2022),**12540-12550, Doi: 10.1039/D2NJ02170F.

[26] F. Tisato, C. Marzano, M. Porchia, M. Pellei, C. Santini, Med. Res. Rev. 30 (2010) 708–749, https://doi.org/10.1002/med.20174. C. Santini, M. Pellei, V. Gandin, M. Porchia, F. Tisato, C. Marzano. *Chem. Rev.*, 114, **(2014),** 815-862, Doi: 10.1021/cr400135x; K. Dankhoff, M. Gold, L. Kober, F. Schmitt, L. Pfeifer, A. Dürrmann, H. Kostrhunova, M. Rothemund, V. Brabec, R. Schobert, B. Weber *Dalton Trans.*, 48, **(2019)**, 15220-15230, Doi: 10.1039/c9dt02571e; D. A. da Silva, A. de Luca, R. Squitti, M. Rongioletti, *L. Rossi*, C. M.L. Machado, G. Cerchiaro *J. Inorg. Biochem.* 226, **(2022)**, 111634, Doi: 10.1016/j.jinorgbio.2021.111634.

[27] C. Duncan, A.R. White, Metallomics 4 (2012) 127–138, https://doi.org/10.1039/c2mt00174h.

[28] C. Marzano, M. Pellei, F. Tisato, C. Santini, Anti Cancer Agents Med. Chem. 9 (2009) 185–211, https://doi.org/10.2174/187152009787313837.

[29] L. Ronconi, P.J. Sadler, Coord. Chem. Rev. 251 (2007) 1633–1648, https://doi.org/10.1016/j.ccr.2006.11.017.

[30] R.A. Festa, D.J. Thiele, Curr. Biol. 21 (2011) R877–R883, https://doi.org/10.1016/j.cub.2011.09.040.

[31] S. Lutsenko, E.S. LeShane, U. Shinde, Arch. Biochem. Biophys. 463 (2007) 134–148, https://doi.org/10.1016/j.abb.2007.04.013.

[32] M.E. Helsel, K.J. Franz, Dalton Trans. 44 (2015) 8760–8770, https://doi.org/10.1039/c5dt00634a.

[33] S. Banerjee, P. Ghorai, P. Brandão, D. Ghosh, S. Bhuiya, D. Chattopadhyay, S. Das, A. Saha, New J. Chem. 42 (2018), https://doi.org/10.1039/c7nj03293e, 246–25.

[34] A. Castiñeiras, J.A. Castro, M.L. Durán, J.A. García-Vázquez, A. Macías, J. Romero, A. Sousa, Polyhedron 8 (1989) 2543–2549, https://doi.org/10.1016/S0277-5387(00)81154-7.

[35] J. Viqueira, M.L. Durán, J.A. García-Vázquez, J. Castro, C. Platas-Iglesias, D. Esteban-Gómez, G. Alzuet-Piña, A. Moldes, O.R. Nascimento, New J. Chem. 42 (2018) 15170–15183, https://doi.org/10.1039/c8nj03292k.

[36] I. Beloso, J. Borrás, J. Castro, J.A. García-Vázquez, P. Pérez-Lourido, J. Romero, A. Sousa, Eur. J. Inorg. Chem. (2004) 635–645, https://doi.org/10.1002/ejic.200300338.

[37] C.P. Matos, Y. Addis, P. Nunes, S. Barroso, I. Alho, M. Martins, A.P.A. Matos, F. Marques, I. Cavaco, J.C. Pessoa, I. Correia, J. Inorg. Biochem. 198 (2019), 110727, https://doi.org/10.1016/j.jinorgbio.2019.110727.

[38] A.C. Hangan, R.L. Stan, A. Turza, L.S. Oprean, E. Páll, S. Gheorghe-Cetean, B. Sevastre, Transit. Met. Chem. 42 (2017) 153–164, https://doi.org/10.1007/s11243-017-0120-5.

[39] J.N. Boodram, I.J. Mcgregor, P.M. Bruno, P.B. Cressey, M.T. Hemann, K. Suntharalingam, Angew. Chem. Int. Ed. 55 (2016) 2845–2850, https://doi.org/10.1002/anie.201510443.

[40] S.Y. Ebrahimipour, I. Sheikhshoaie, M. Mohamadi, S. Suarez, R. Baggio, M. Khaleghi, M. Torkzadeh-Mahani, A. Mostafavi, Spectrochim. Acta A 142 (2015) 410–422, https://doi.org/10.1016/j.saa.2015.01.088.

[41] P. Nagababu, A.K. Barui, B. Thulasiram, C.S. Devi, S. Satyanarayana, C.R. Patra, B. Sreedhar, J. Med. Chem. 58 (2015) 5226–5241, https://doi.org/10.1021/acs.jmedchem.5b00651.

[42] A. Rodríguez, J.A. García-Vázquez, Coord. Chem. Rev. 303 (2015) 42–85, https://doi.org/10.1016/j.ccr.2015.05.006.

[43] W.U. Malik, T.C. Sharma, J. Indian Chem. Soc. 47 (1970) 167.

[44] Bruker, Sadabs, Smart, Saint, Bruker AXS Inc., Madison, Wisconsin, USA, 2015.

[45] P. McArdle, J. Appl. Crystallogr. 50 (2017) 320–326, https://doi.org/10.1107/S1600576716018446.

[46] G.M. Sheldrick, Acta Crystallogr. A 71 (2015) 3–8, https://doi.org/10.1107/S2053273314026370.

[47] G.M. Sheldrick, Acta Crystallogr. C 71 (2015) 3–8, https://doi.org/10.1107/S2053229614024218.

[48] J. Kovalevich, D. Langford, Methods Mol. Biol. 1078 (2013) 9–21, https://doi.org/10.1007/978-1-62703-640-5_2.

[49] H. Motaln, A. Koren, K. Gruden, Z. Ramsak, C. Schichor, T.T. Lah, Oncotarget 6 (2015) 40998–41017, https://doi.org/10.18632/oncotarget.5701.

[50] J. van Meerloo, G.J.L. Kaspers, J. Cloos, Methods Mol. Biol. 731 (2011) 237–245, https://doi.org/10.1007/978-1-61779-080-5_20.

[51] I. Marrocco, F. Altieri, I. Peluso, Oxidative Med. Cell. Longev. (2017) 6501046, https://doi.org/10.1155/2017/6501046, 2017.

[52] J. Metz, O. Schneider, M. Hanack, Spectrochim. Acta A 38 (1982) 1265–1273, https://doi.org/10.1016/0584-8539(82)80124-4.

[53] R.G. Inskeep, J. Inorg. Nucl. Chem. 24 (1963) 763–776, https://doi.org/10.1016/0022-1902(62)80096-7.

[54] A.A. Schilt, R.C. Taylor, J. Inorg. Nucl. Chem. 9 (1959) 211–221, https://doi.org/10.1016/0022-1902(59)80224-4.

[55] A.B.P. Lever, Inorganic Electronic Spectroscopy, 2nd edn, Elsevier, Amsterdan, 1984.

[56] L.J. Farrugia, J. Appl. Crystallogr. 45 (2012) 849–854, https://doi.org/10.1107/S0021889812029111. POV-Ray v3.7 for Windows, Persistence of Vision Pty. Ltd. (2016) Persistence of Vision Raytracer (Version 3.7) retrieved from http://www.povray.org/download/.

[57] P. Müller, Crystallogr. Rev. 15 (2009) 57–83, https://doi.org/10.1080/08893110802547240.

[58] D.M. Tooke, A.L. Spek, Acta Crystallogr. E 60 (2004) o766–o767, https://doi.org/10.1107/S160053680400830X.

[59] N. Özdemir, R. Kağıt, O. Dayan, Mol. Phys. 114 (2016) 757–768, https://doi.org/10.1080/00268976.2015.1116715.

[60] F.H. Allen, O. Kennard, D.G. Watson, L. Brammer, A.G. Orpen, R. Taylor, J. Chem. Soc. Perkin II (1987) S1–S19, https://doi.org/10.1039/P298700000S1.

[61] J.J. MacKinnon, M.A. Spackman, A.S. Mitchell, Acta Crystallogr. B 60 (2004) 627–668, https://doi.org/10.1107/S0108768104020300. M. A. Spackman, D. Jayatilaka CrystEngComm, 11, (2009), 19–32, Doi: 10.1039/b818330a.

[62] S.K. Wolff, D.J. Grimwood, J.J. McKinnon, M.J. Turner, D. Jayatilaka, M. A. Spackman, CrystalExplorer (Version 3.1), University of Western Australia, Perth, Australia, 2022. www.hirshfeldsurface.net.

[63] A.L. Spek, Acta Crystallogr. D 65 (2009) 148–155, https://doi.org/10.1107/S090744490804362X.

[64] L. Yang, D.R. Powell, R.P. Houser, Dalton Trans. (2007) 955–964, https://doi.org/10.1039/B617136B. A. Okuniewski, D. Rosiak, J. Chojnacki, B. Becker Polyhedron 90, (2015), 47–57, Doi: 10.1016/j.poly.2015.01.035.

[65] V.M. Leovac, L.S. Vojinović-Ješić, V.I. Češljević, S.B. Novaković, G.A. Bogdanović, Acta Crystallogr. C 65 (2009) m337–m339, https://doi.org/10.1107/S0108270109029023.

[66] Z.-L. You, Acta Crystallogr. E62 (2006), m1207, https://doi.org/10.1107/S1600536806016175.

[67] D. de Bellefeuille, M. Orio, A.-L. Barra, A. Aukauloo, Y. Journaux, C. Philouze, X. Ottenwaelder, F. Thomas, Inorg. Chem. 54 (2015) 9013–9026, https://doi.org/10.1021/acs.inorgchem.5b01285. P. K. Bhaumik, A. Bauzá, M. G. B. Drew, A. Frontera, S. Chattopadhyay CrystEngComm, 17, (2015), 5664–5671, Doi: 10.1039/C5CE00809C; S.-N. Li, Q.-G. Zhai, M.-C. Hu, Y.-C. Jiang J. Coord. Chem., 62, (2009), 2709–2718, Doi: 10.1080/00958970902912373; Y.-M. Yang Acta Cryst. E61, (2005), m1425-m1426, Doi: 10.1107/S1600536805019975.

[68] A.W. Addison, T.N. Rao, J. Reedijk, J. van Rijn, G.C. Verschoor, J. Chem, Soc. Dalton Trans. (1984) 1349–1356, https://doi.org/10.1039/DT9840001349. A. G. Blackman, E. B. Schenk, R. E. Jelley, E. H. Krensked, L. R. Gahan Dalton Trans., 49, (2020),14798–14806, Doi: 10.1039/d0dt02985h.

[69] M. Rivera-Carrillo, I. Chakraborty, R.G. Raptis, Cryst. Growth Des. 10 (2010) 2606–2612, https://doi.org/10.1021/cg100060p. C. Jia, Q. Lin, W. Yuan CrystEngComm, 16, (2014), 2508-2519, Doi: 10.1039/C3CE42127A.

[70] C. Stefani, Z. Al-Eisawi, P.J. Jansson, D.S. Kalinowski, D.R. Richardson, J. Inorg. Biochem. 152 (2015) 20–37, https://doi.org/10.1016/j.jinorgbio.2015.08.010.

[71] K. Konarikova, J. Frivaldska, H. Gbelcova, M. Sveda, T. Ruml, M. Janubova, I. Zitnanova, Bratisl. Lek. Listy 120 (2019) 646–649, https://doi.org/10.4149/bll_2019_107.

[72] G. Filomeni, S. Cardaci, A.M. Da Costa Ferreira, G. Rotilio, M.R. Ciriolo, Biochem. J. 437 (2011) 443–453, https://doi.org/10.1042/bj20110510.

[73] C. Olivier, L. Olivier, L. Lalier, F.M. Vellette, Front. Mol. Biosci. 7 (2021) 620677, https://doi.org/10.3389/fmolb.2020.620677.

[74] M. Hajrezaie, M. Paydar, S.Z. Moghadamtousi, P. Hassandarvish, N.S. Gwaram, M. Zahedifard, E. Rouhollahi, H. Karimian, C.Y. Looi, H.M. Ali, N.A. Majid, M. A. Abdull, Sci. World J. (2014), 540463, https://doi.org/10.1155/2014/540463.

[75] L.W. Ki, J.E. Lee, J.H. Park, I.C. Shin, H.C. Koh, Toxicol. Lett. 211 (2012) 18–28, https://doi.org/10.1016/j.toxlet.2012.02.022.

[76] D. Goldschneider, E. Blanc, G. Raguénez, M. Barrois, A. Legrand, G. Le Roux, H. Haddada, J. Bénard, S. Douc-Rasy, J. Cell Sci. 117 (2004) 293–301, https://doi.org/10.1242/jcs.00834.

[77] D. Goldschneider, E. Horvilleur, L.-F. Plassa, M. Guillaud-Bataille, K. Million, E. Wittmer-Dupret, G. Danglot, H. de Thé, J. Bénard, E. May, S. Douc-Rasy, Nucleic Acids Res. 34 (2006) 5603–5612, https://doi.org/10.1093/nar/gkl619.

[78] S. Surget, M.P. Khoury, J.-C. Bourdon, OncoTargets Ther. 7 (2014) 57–68, https://doi.org/10.2147/ott.s53876.

[79] E.G. Van Meir, T. Kikuchi, M. Tada, H. Li, A.C. Diserens, B.E. Wojcik, H.-J. Su Huang, T. Friedmann, N. de Tribolet, W.K. Cavenee, Cancer Res. 54 (1994) 649–652.

[80] S.A. Moallem, B.F. Hales, Development 125 (1998) 3225–3234, https://doi.org/10.1242/dev.125.16.3225.

[81] W. Chaabane, S.D. Use, M. El-Gazzah, R. Jaksik, E. Sajjadi, J. Rzeszowska-Wolny, M.J. Los, Arch. Immunol. Ther. Exp. 61 (2013) 43–58, https://doi.org/10.1007/s00005-012-0205-y.

[82] J. Lou, Y. Zhou, Z. Feng, M. Ma, Y. Yao, Y. Wang, Y. Deng, Y. Wu, Front. Oncol. 10 (2021), 616952, https://doi.org/10.3389/fonc.2020.616952.